J. Appl. Comput. Mech., 4(4) (2018) 375-401
DOI: 10.22055/JACM.2018.25686.1286

ISSN: 2383-4536
jacm.scu.ac.ir

Shahid Chamran University of Ahvaz

Journal of Applied and Computational Mechanics

Review Paper

A Review of Solar Energy Collectors: Models and Applications

Younes MENNI[1], Ahmed AZZI[1,2], Ali CHAMKHA[3,4]

[1] Unite of Research on Materials and Renewable Energies - URMER - Department of Physics, Faculty of Sciences, Abou Bekr Belkaid University BP 119-13000-Tlemcen, Algeria

[2] Department of Mechanical Engineering, Faculty of Technology, Abou Bekr Belkaid University BP 230-13000-Tlemcen, Algeria

[3] Mechanical Engineering Department, Prince Sultan Endowment for Energy and Environment, Prince Mohammad Bin Fahd University Al-Khobar 31952, Saudi Arabia

[4] RAK Research and Innovation Center, American University of Ras Al Khaimah, P.O. Box 10021, Ras Al Khaimah, United Arab Emirates

Received April 28 2018; Revised June 16 2018; Accepted for publication June 16 2018.
Corresponding author: Ali CHAMKHA, achamkha@pmu.edu.sa

Abstract. A current study and discussion in detail about many solar energy collectors of various types, components, classifications and configurations, through the analysis of their performance, is our aim through this review paper. The effects of the geometrical parameters of the solar air collectors as well as the functioning parameters on heat transfer and fluid flow processes were also discussed in detail. The numerical, analytical, and experimental analyses on different models of flat plate solar air collectors with various thermal transfer enhancement strategies were shown in various stages, i.e., modelling, control, measurement, and visualization of airfield, determination of heat transfer, control of friction loss and pressure drop, and evaluation of the thermal performance by the measurement of the augmentation in the temperature of the working fluid at a given solar irradiance and under given flow rate. We concluded this review by identifying the various applications possible for the solar air collectors such as heating and cooling of houses, drying agricultural food materials, and water desalination process.

Keywords: Solar energy collector; Flat absorber; Single-pass solar air collector; Double-pass solar air collector; Applications of air solar collectors.

1. Introduction

Solar energy collector is a special type of heat exchanger that transforms solar radiation energy into internal energy of the transport medium. Basically, there are two types of flat-plate solar heating collectors; water heating collectors and air heating collectors. The pace of development of air heating collector is slow compared to water heating collector mainly due to lower thermal efficiency. Solar air collectors are widely used for low to moderate temperature applications like space heating, crop drying, timber seasoning and other industrial applications. Conventional solar air collectors have poor thermal efficiency principally due to high heat losses and low convective heat transfer coefficient between the absorber plate and flowing air stream. Attempts have been made to improve the thermal performance of conventional solar air collectors by employing various design and flow arrangements (Ramani et al., 2010 [1]).

2. Single-pass flat plate solar air collectors

Several researchers have investigated the solar air collectors numerically and experimentally to enhance the performance.

Deng et al. (2015) [2] analyzed the thermal performance of a single-pass flat plate solar air collector (SAC) in the case of severe dust deposition surface, see Fig. 1. Experiments of the SAC with both severe dust deposition surface and clean cover surface were conducted using the steady-state test (SST) method, in order to show a contrast. The mathematical relation between the combined standard uncertainty of the predicted thermal efficiency and the uncertainties of the experimental results was presented. And the collector characteristic parameters, such as the collector heat removal factor, the collector flow efficiency factor, the total heat loss coefficients, etc. were obtained. The results showed that, the predicted thermal efficiency in the case of severe dust deposition surface is decreased by 10.7% - 21.0% when the normalized temperature difference ranges from 0 to 0.04. And the optical efficiency of the SAC is decreased by 8.39% when the collector transparent glass cover is under the condition of severe dust deposition.

(a) **(b)**

Fig. 1. The cases of the flat-plate SAC (a) clean surface, (b) severe dust deposition [2].

Moss et al. (2018) [3] demonstrated the reduction in heat loss coefficient and increase in efficiency resulting from evacuating a flat plate collector: it is hoped that these results will stimulate interest in the concept. Evacuated tubes are now mass-produced in large numbers; evacuated flat plate collectors could in principle replace these tubes if the technical difficulties in creating extended metal-glass seals can be overcome. The experimental experiences described here should indicate targets for future research.

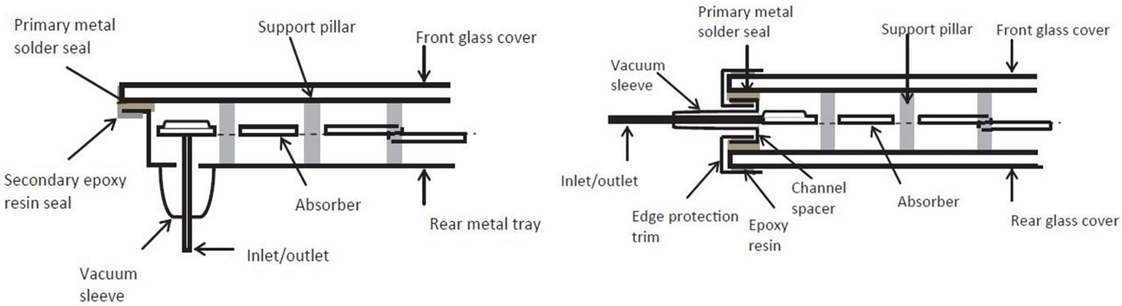

(a) **(b)**

Fig. 2. Cross-sections of the collectors. (a) Collector P1 (with rear tray), (b) Collector F1 (symmetrical) [3].

Two styles (P1 and F1) of vacuum enclosure were tested, see Fig. 2. Both performed well and demonstrated a very significant efficiency increase between ambient and evacuated conditions. 4mm toughened glass with a 60 mm pitch pillar array provided a sufficient safety margin even when a few pillars were missing. The tray-based enclosure was more flexible than the symmetrical design and more resistant to thermal stress-induced leakage.

Zhu et al. (2017) [4] proposed a new type of a flat-plate solar air collector (SAC) with micro-heat pipe arrays (MHPA), which consist of a heat collection and transfer section and an air ventilation and heat exchange section, see Fig. 3. They experimentally and theoretically investigated the heat transfer and friction factor characteristics of the proposed MHPA-flat plate solar air collector. Numerical simulation and experimental results were compared to show the instantaneous performance of the collector under quasi-steady state conditions. Efficiency, time constant, inlet temperature, outlet temperature, absorber temperature, and glass cover temperature were obtained. The effects of weather condition, and operational parameters were evaluated on the basis of thermal efficiency, outlet temperature, heat loss, and heat transfer. Results showed that the average efficiency is approximately 69% at a flow rate of 290 m3/h. In the testing range of the air flow rate, the frictional coefficient varied from 0.05 to 0.18.

Lingayat et al. (2018) [5] developed a 2D numerical model in order to study the heat transfer and fluid mechanics phenomenon inside the solar collector of an indirect type solar dryer (ITSD) where the absorber plate of collector is provided with square roughness, see Fig. 4. ANSYS FLUENT v16 was used to simulate the problem domain. Effects of *Re* number, velocity, relative roughness height (*e/D*), relative roughness pitch (*P/e*) on heat transfer coefficient *(h)* and frictional factor were studied. Presented model was validated with experimental data available in the literature and found good agreement.

Abuşka and Şevik (2017) [6] carried out an experimental investigation to study the effect of energy, economic, and environment of SACs which are smooth and roughened by v-groove protrusions arranged made of copper and aluminium materials, see Fig. 5. In this context; energy, exergy, economic, and environment (4E) analyses were investigated using data obtained from experimental studies at air mass flow rates of 0.04, 0.06, 0.08 and 0.1 kg/s. Thermal, economic, and environmental impacts for performance enhancement of the SACs were determined. As expected, experimental results showed that the v-grooved surface has the better efficiency than flat SAC.

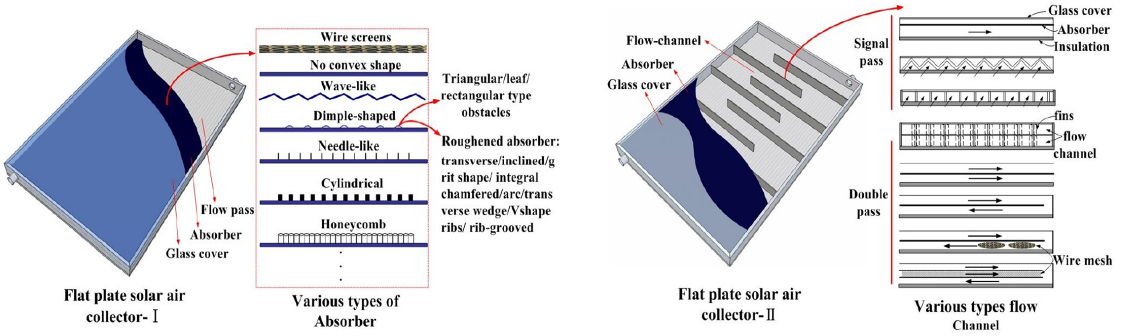

(a) **(b)**

Fig. 3. Representative flat-plate SACs with (a) roughness elements or (b) increased turbulence [4].

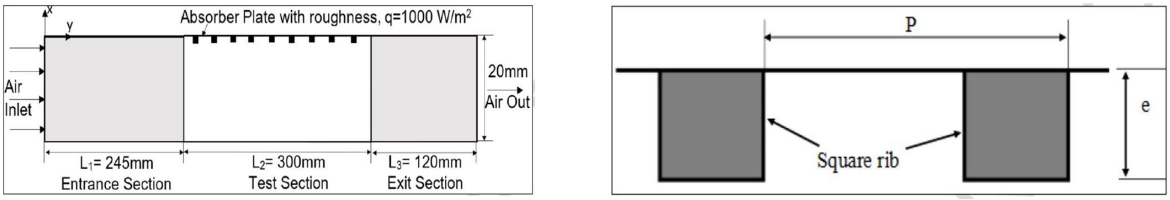

(a) **(b)**

Fig. 4. (a) 2D computational domain for square rib and (b) enlarged view of roughened absorber plate with square-shaped rib [5].

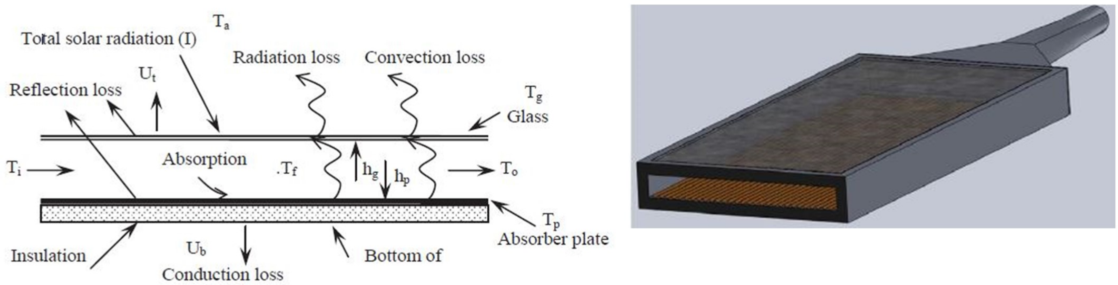

(a) **(b)**

Fig. 5. (a) Heat transfer model and thermal network of a SAC, (b) Photograph of the solar air collector [6].

Saedodin et al. (2017) [7] carried experimental and numerical investigations on the effect of porous metal foam on the performance of a flat-plate solar collector, see Fig. 6. The numerical solution is based on the control-volume approach and local thermal equilibrium assumption between the fluid-porous material phase to get the optimum thickness of the porous medium and also evaluate the thermal performance and pressure drop in the porous channel collector. The numerical and experimental results have shown that using the porous medium enhances the maximum thermal efficiency and Nusselt number up to 18.5% and 82%, respectively.

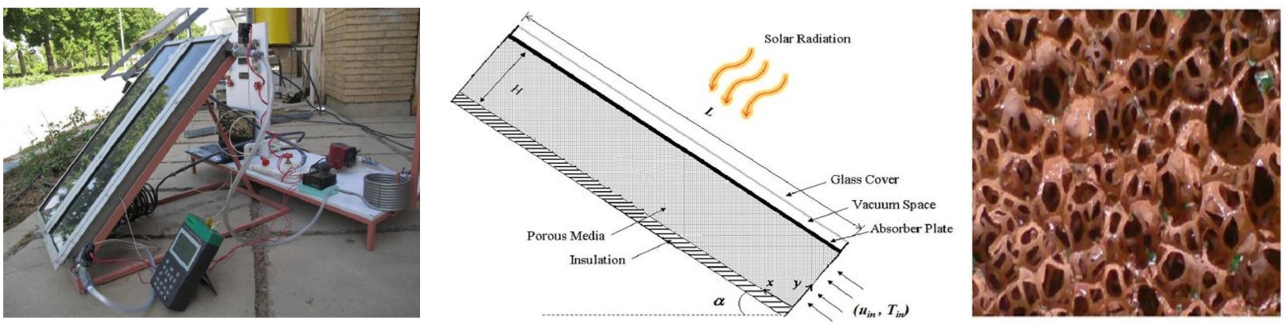

(a) **(b)** **(c)**

Fig. 6. (a) Experimental setup, (b) A schematic diagram of the porous channel FPSC and its coordinates, (c) A photograph of the copper metal foam (cellular arrangement) [7].

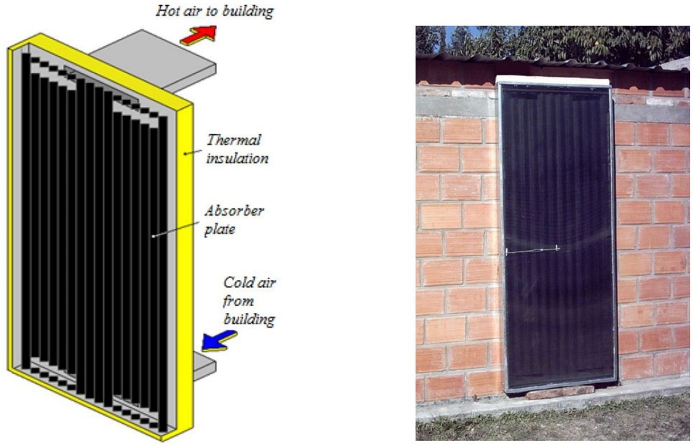

(a) **(b)**

Fig. 7. (a) Schematic section of solar collector, (b) Solar air collector installed for testing [8].

Hernández and Quiñonez (2017) [8] presented the experimental validation of an analytical model that describes the thermal behaviour of double parallel flow air heating collectors working by natural convection, see Fig. 7. This model was validated with data measured on a collector of these characteristics at the National University of Salta, in the northwest of Argentina. Comparisons between measured and simulated values showed an excellent agreement for both the air output temperature and the useful energy produced by the collector, with RMSE values smaller than 6 %. The instantaneous thermal efficiency curve of the collector was determined experimentally in winter of 2015. Daily values of efficiency ranged between 0.48 and 0.5 during sunny days and between 0.41 and 0.46 during semi-cloudy days. A novel correlation between the velocity of the air movement by natural convection and the temperature difference between the building and the collector's interior was obtained by means of linear regression with a correlation coefficient R2 = 0.94. A new correlation $Nu = f(Ra)$ to estimate the average convective coefficients by natural convection was obtained, based on an effective convective heat transfer coefficient calculated with the temperature values measured inside the collector and the absorbed solar irradiance.

(a) **(b)**

Fig. 8. (a) Photographic view of modified (left) and conventional (right) solar air heater, (b) Arrangement of turbulators in absorber plate [9].

Rajaseenivasan et al. (2015) [9] performed a detailed theoretical and experimental study to evaluate the capacity of the single pass SAH with six patterns of turbulators, i.e., inline arrangements with 4 × 4 (type-a), 5 × 4 (type-b), 6 × 4 (type-c) and 6 × 4 zigzag arrangement of circular inserts (type-d), in the absorber plate with a wide range of operating conditions. A conventional SAH was simultaneously experimented with modified SAH for comparison purpose, see Fig. 8. Theoretical results were compared with experimental results and the deviations were within 10 %. Experiment results revealed that the system efficiency increases with Reynolds number and number of turbulators in absorber plate. Air temperature reaches an upper value of 66 °C in type-f with the mass flow rate of 57.7 kg/hr. Nusselt number increases with the Reynolds number and reaches the maximum of 210 for type-f turbulators at Reynolds number of 11615. Thermal enhancement factor decreases with increase in Reynolds number for all modifications. First law, thermohydraulic and second law efficiency increases up to 85%, 63% and 45% respectively for type-f at Reynolds number of 11615. Theoretical analysis also carried out and agrees well with experimental results.

Abuşka (2017) [10] investigated and compared the thermal performance of a new design absorber plate with conical surface to flat absorber plate in single front pass conventional solar air heater, see Fig. 9. The aim of the survey is to propose a more efficient absorber plate with low-pressure drop relatively, to increase the amount of energy obtained, to decrease the cost of energy provided by the sun, and to use it by sustainably. The experiments were performed for three mass flow rates of 0.04, 0.08, and 0.10 kg/s in outdoor conditions. The average thermal efficiency is obtained as 63.2-57.2% for 0.04, 71.5-61.7% for

0.08, and 74.6-64.0% for 0.1 kg/s in conical and flat absorber plate, respectively. The highest thermal efficiency was determined for the solar air heater with conical surface for all operating conditions.

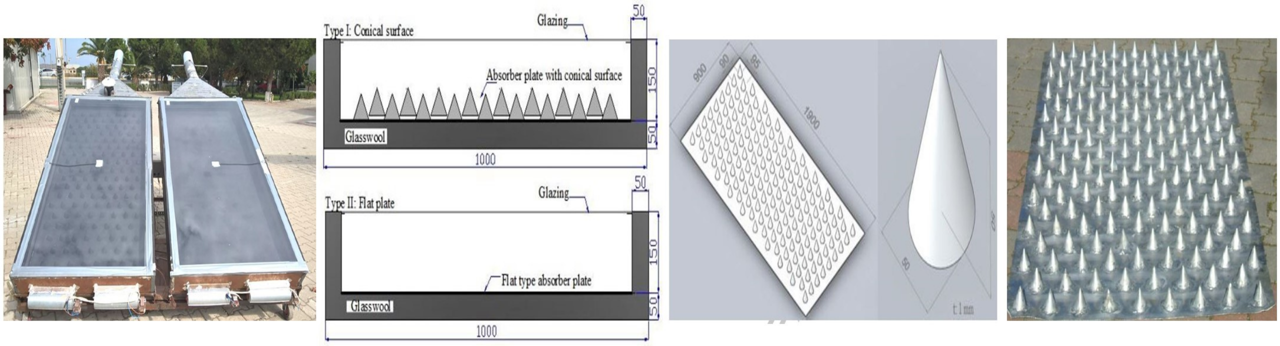

(a) **(b)** **(c)** **(d)**

Fig. 9. (a) Experimental setup, (b) Sectional view of the heaters, (c) Drawing of the absorber plate with conical surface, and (d) The absorber plate image [10].

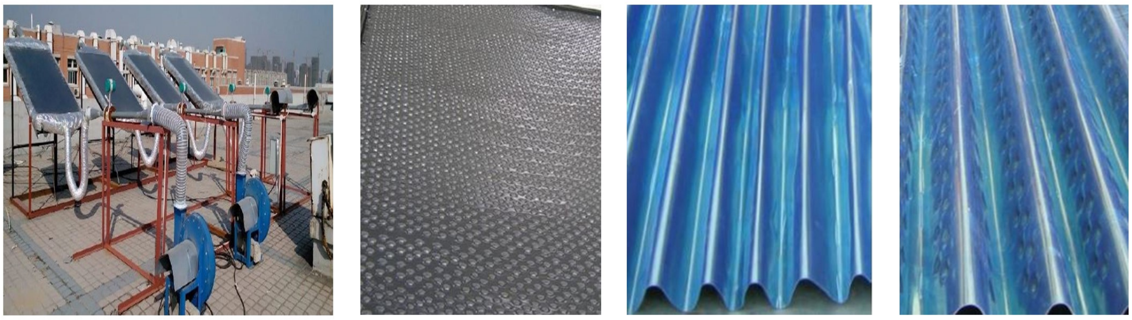

(a) **(b)**

Fig. 10. (a) The test system of solar air collector, (b) The absorbers with different structure [11].

Li et al. (2016) [11] presented an experimental investigation on the absorber surface of the collector whose shape to provide better heat transfer surfaces, see Fig. 10. In this study four types of air solar collectors: sinusoidal corrugated plate, protrusion plate, sinusoidal corrugated and protrusion plate and a base flat-plate collector were presented. The results of the experiments were evaluated at the same time of the days with the same radiation. The efficiencies were determined for the collectors and comparisons were made among them. The present data showed that heat transfer coefficient and pressure drop and the performance factor PF increase with shape of absorbers surface.

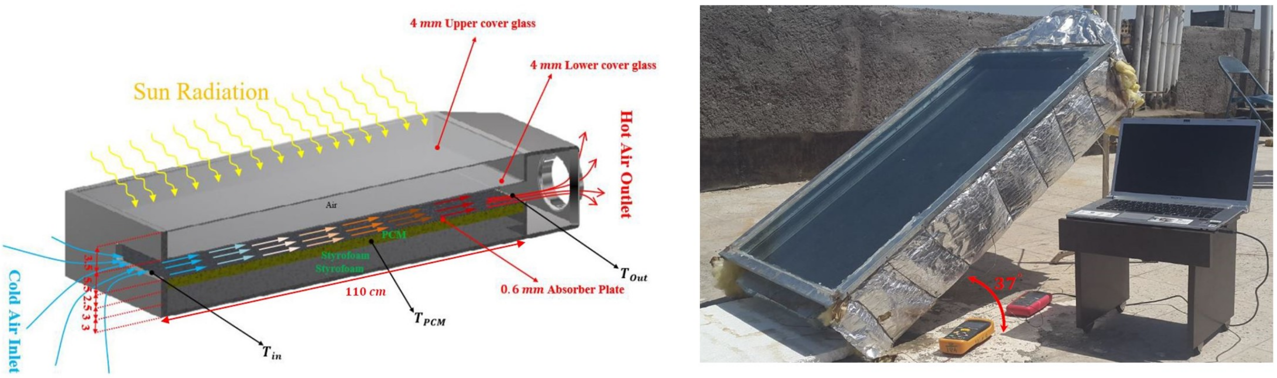

(a) **(b)**

Fig. 11. (a) Cross sectional view of SAH without baffles, (b) SAH set up [12].

Ghiami and Ghiami (2017) [12] evaluated experimentally a novel baffle-equipped SAH with integrated storage unit (PCM cavity) in terms of its performance, under the meteorological conditions of Mashhad, Iran, see Fig. 11. The characteristics of the system were scrutinized in presence and absence of baffle on the absorber plate. In the experimental study, two types of baffle-equipped and an unequipped absorber plate were inspected in presence of PCM unit and their exergy and efficiency were compared. For the baffled absorber plates, the baffles are made of galvanized plates and are arranged in sequential or staggered manner. They showed that, at the mass flow rate of 0.017 Kg/s, the maximum energy efficiency was attained for sequence-arranged baffle-equipped SAH (26.78%), while unequipped SAH had the least energy efficiency (14.30%) at the same mass flow rate. The exergy efficiencies varied between 4.86 - 20.47 % for all cases of study.

Chen et al. (2015) [13] investigated full-scale traditional metal solar collectors and solar collector specimens fabricated from polymeric materials, see Fig. 12. A polymeric collector is 67.8% lighter than a traditional metal solar collector, and a metal solar collector with transparent plastic covering is 40.3% lighter than a traditional metal solar collector. Honeycomb multichannel plates made from polycarbonate were chosen to create a polymeric solar collector. A test rig for the natural circulation of the working fluid in a solar collector was built for a comparative experimental investigation of various solar collectors operating at ambient conditions. It was shown experimentally that the efficiency of a polymeric collector is 8 -15% lower than the efficiency of a traditional collector. The results of a Life Cycle Assessment study showed the advantages of the application of polymeric materials in the construction of solar collectors.

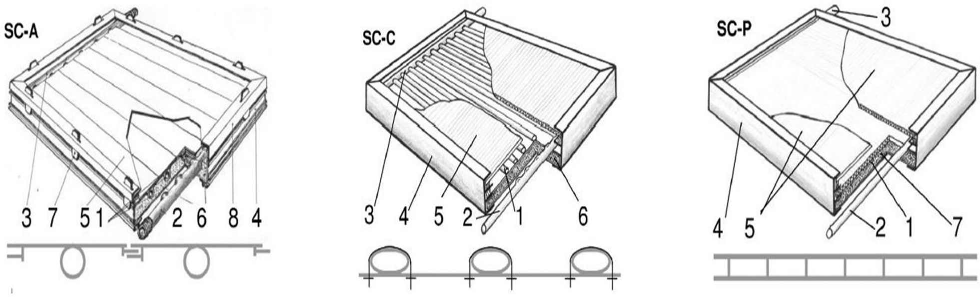

Fig. 12. General views of the studied solar collectors: 1 - absorber; 2, 3 - hydraulic collectors; 4 - frame, 5 - transparent cover; 6 – thermal insulation; 7 - bottom; 8 - fastening element [13].

Kabeel et al. (2017) [14] experimentally investigated the thermal performance of the finned plate solar air heater (FPSAH) using paraffin wax as phase change material (PCM), see Fig. 13. The proposed collector was manufactured and tested under weather circumstances of Tanta town (30° 47/ N, 31°E), Egypt. The effect of changing the mass flow rate on the instantaneous and daily efficiencies was also investigated. The influence of changing the mass of the PCM on the performance of the heater was also studied. The experimental results showed that the instantaneous and daily efficiencies of the FPSAH with and without using the PCM increases when the mass flow rate increases on the expense of the outlet temperature as it decreases. It is also found that the operation of the FPSAH extended up to 4 hours after sunset with outlet temperature reach 8.6 ºC more than ambient when 39 kg of paraffin wax is used as latent heat storage. Depends on the results displayed in this study it is explored that using the PCM by the FPSAH improves the daily efficiency by 10.8-13.6%.

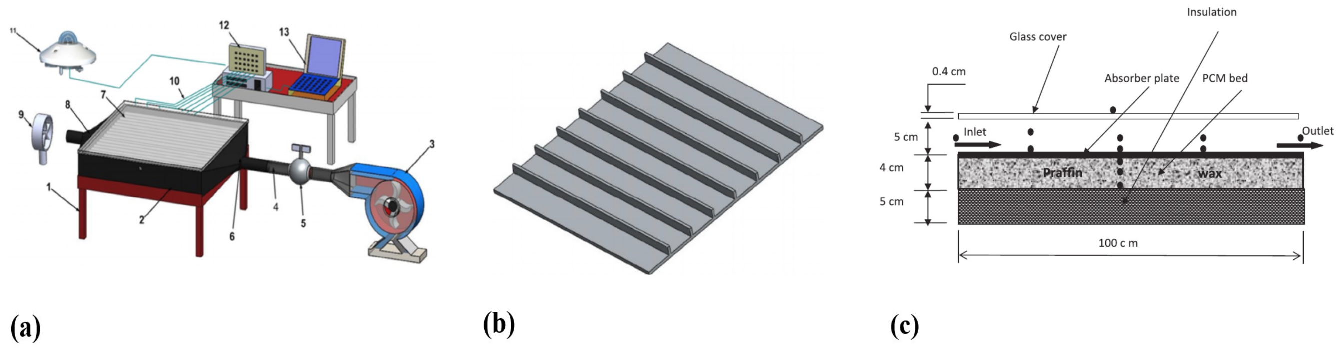

Fig. 13. (a) A schematic diagram of the experimental setup, (b) Configuration of the finned absorber plate, (c) Section view of the SAH and the PCM channel [14].

Kalaiarasi et al. (2016) [15] conducted a comparative experimental investigation of SAH with and without a special designed integrated absorber-cum-sensible heat storage unit at Madurai city in India, see Fig. 14. Their performance were analyzed based on both energy and exergy efficiencies. Both the SAHs were tested from 10:00 - 18:00 h IST for two different mass flow rates, $\dot{m}$ = 0.018 kg/s and 0.026 kg/s. The results showed that the maximum energy and exergy efficiency obtained was in the range of 49.4 - 59.2 % and 18.25 - 37.53 % respectively, for the SAH with sensible storage at $\dot{m}$ = 0.026 kg/s. Besides, the SAH with sensible heat storage was observed to perform better than the conventional flat plate SAH without storage.

Mohammadi and Sabzpooshani (2013) [16] investigated the influence of fins and baffles attached over the absorber plate on the performance of the upward type single pass solar air heater, see Fig. 15. A steady-state mathematical model was presented and solved theoretically. The performance evaluation was studied in terms of different performance indicators, such as outlet air temperature, efficiency and effective efficiency. They found that attaching fins and baffles effectively increases the outlet air temperature and efficiency in comparison to a simple conventional device. However, they observed that increasing the number of fins and baffles parameters can reduce effective efficiency even less than a simple conventional device in some cases due to the high required pump work.

Mohammadi and Sabzpooshani (2014) [17] aimed at appraising the possibility of enhancing thermal performance of an upward-type single pass solar air heater by utilizing fins and baffles over the absorber plate, see Fig. 16, as well as applying external recycle device simultaneously under various parametric conditions. The energy and effective efficiencies analysis was used as criteria to evaluate the performance. The investigation was carried out for three cases: simple absorber plate, absorber plate with fins and absorber plate with fins and baffles. The achieved results disclosed that attaching both fins and baffles to the absorber plate under external recycling operation is an effective method to boost the energy efficiency notably. In contrast, the effective efficiency analysis revealed that attaching both fins and baffles at high mass flow rates and recycle ratios leads to considerable decline in effective efficiency. Parametric studies on variation of baffle parameters illustrated that increasing the baffles width as well as declining the distance between baffles under turbulent flow regime is not economically feasible owing to extremely increase of the pressure drop and required pump work. In a nutshell, they found that utilizing only fins under external recycle application at high mass flow rates and recycle ratios is an attractive option.

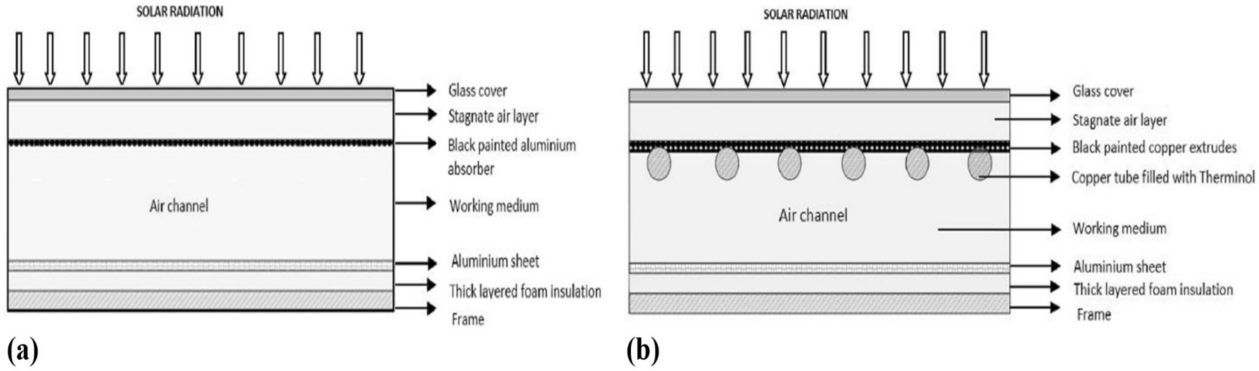

Fig. 14. (a) Cross sectional view of type-I SAH, (b) Cross sectional view of type-II SAH [15].

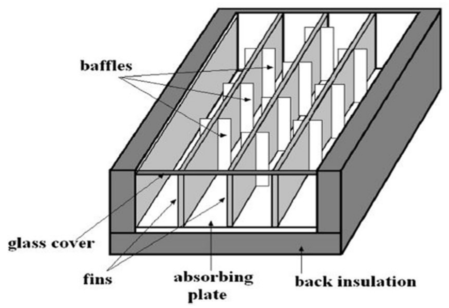

Fig. 15. Schematic diagram of a single pass upward type solar air heater with fins and baffles attached over the absorber plate [16].

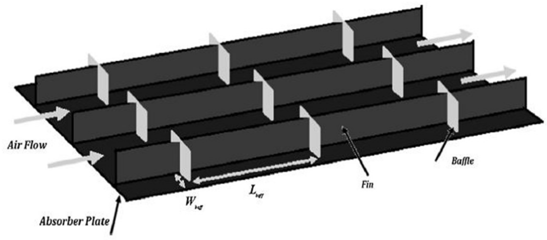

Fig. 16. Schematic view of the absorber plate with attached fins and baffles [17].

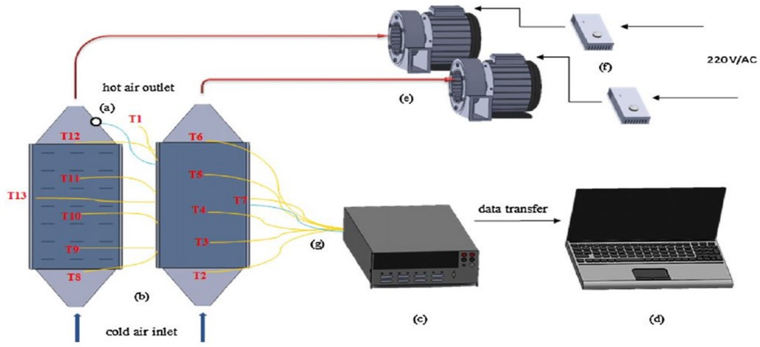

Fig. 17. A schematic view of the experimental set-up, (a) pyranometer, (b) solar air collectors, (c) data logger, (d) computer, (e) radial fans, (f) speed control devices, and (g) thermocouples [18].

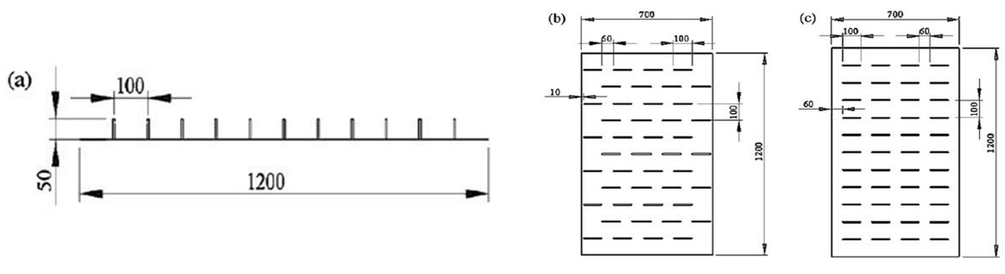

Fig. 18. Various views of the aluminum foams (a) side view of the sequence and staggered arrays, (b) top view of the staggered array, and (c) top view of the sequence array [18].

Bayrak et al. (2013) [18] examined the heat transfer enhancement effectiveness using porous baffles in a solar air heater at different flow rates, different types of porous baffles and location of baffles, see Figs. 17 and 18. They determined energy and exergy efficiencies through energy and exergy analyses, and investigated sustainability assessment values parametrically and relative CO2 reduction potential values comprehensively. The obtained results showed that the highest collector efficiency and air temperature rise are achieved by SAHs with a thickness of 6 mm and an air mass flow rate of 0.025 kg/s whereas the lowest values are obtained for the SAH with non-baffle collectors and an air mass flow rate of 0.016 kg/s.

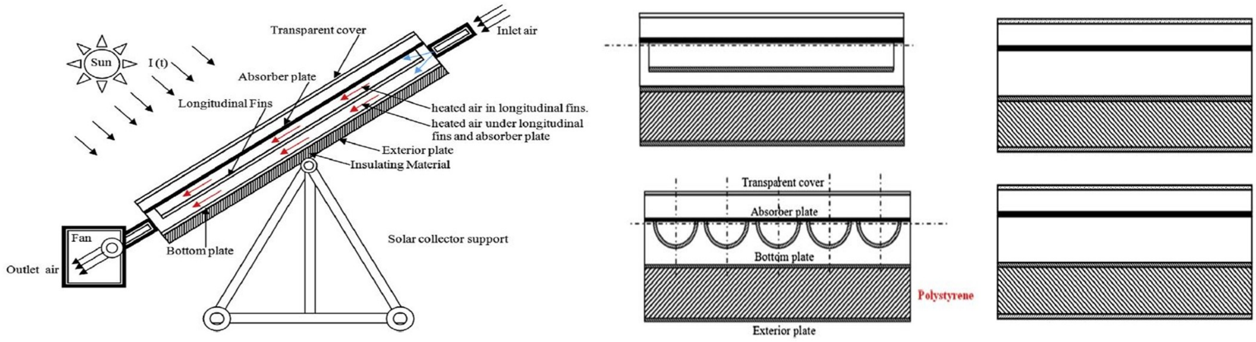

(a) **(b)**

Fig. 19. (a) Schematic view of the solar air collector, (b) Composition of a solar box with and without fins [19].

Chabane et al. (2013) [19] experimentally investigated the thermal performance of a single pass solar air heater with five fins attached, see Fig. 19. Longitudinal fins were used inferior the absorber plate to increase the heat exchange and render the flow fluid in the channel uniform. The effect of mass flow rate of air on the outlet temperature, the heat transfer in the thickness of the solar collector, and the thermal efficiency were studied. A comparison of the results of the mass flow rates by solar collector with and without fins showed a substantial enhancement in the thermal efficiency.

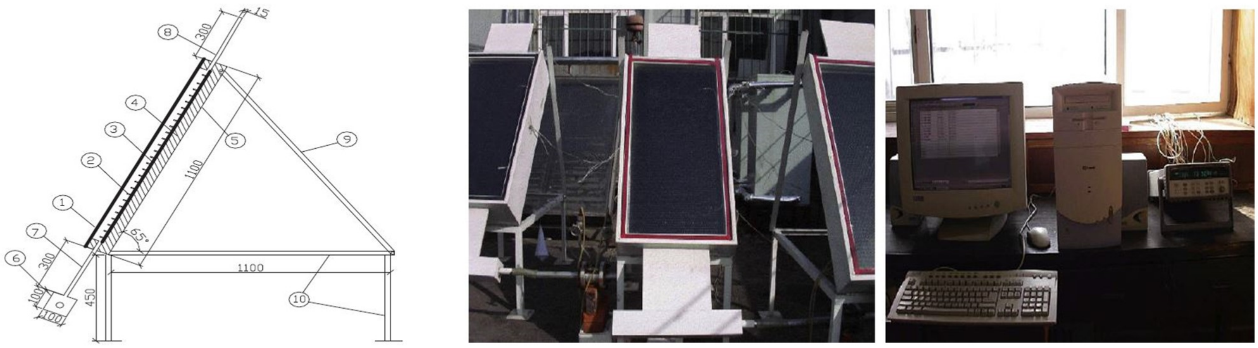

(a) **(b)**

Fig. 20. (a) Configuration of pin-fin arrays solar air collector, (b) Left: Photograph of examined solar air collector in the experimental site. Right: Photograph of test and data acquisition system [20].

Peng et al. (2010) [20] designed a novel solar air collector of pin-fin integrated absorber to increase the thermal efficiency, see Fig. 20. According to experimental results, the average thermal efficiency of twenty-five kinds of pin-fin arrays collector reach 0.5 - 0.74 compared to the solar transmittance of 0.83 for the glazing.

Hu et al. (2013) [21] aimed to investigate a simple-structure mechanical ventilation solar air collector (MV-SAC) with internal baffles, see Fig. 21.

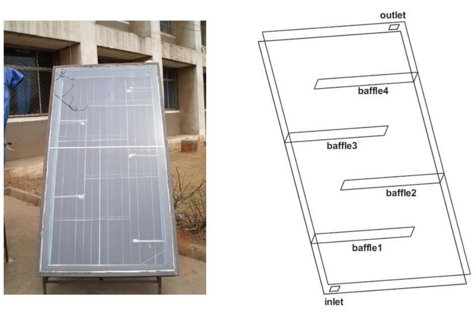

(a) **(b)**

Fig. 21. (a) Photo of the solar air collector, (b) Four-baffle SAC computational model [21].

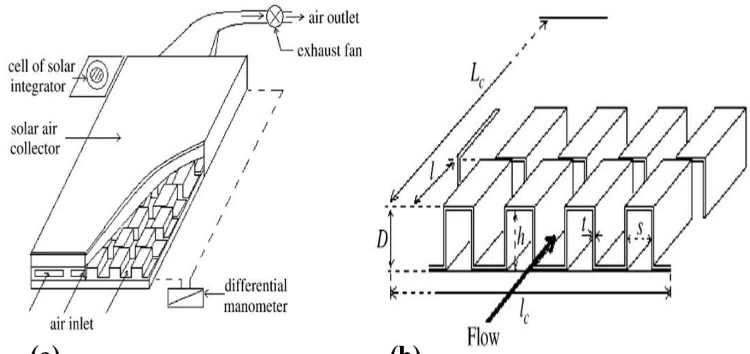

(a) **(b)**

Fig. 22. (a) Experimental setup, (b) Offset rectangular plate fin absorber plate [22].

A numerical model was developed to predict its internal flow and heat transfer characteristics. And a sample experimental system was built and tested for validation of the numerical model. The investigation results indicated that the introduction of baffles can strengthen the convective heat transfer process and lessen the radiation heat loss, which contributes to efficiency improvement. But the presence of baffles causes strong flow separation which results in flow loss to some extent. The convective heat loss of the top cover plate is dominative in the total heat loss. The influence of baffle number, the thickness of air gap, the number of top glass cover and the operating conditions on the collector performance was also analyzed, and the results showed that as for a specific scale collector, there exists an optimal baffle number, for this case the number is three. The operating parameters such as the surrounding temperature, solar radiation intensity have significant influence on the temperature rise but have little influence on collector efficiency, which indicates that this kind of solar air collector could be applied in a wide range of geographical latitude.

Youcef-Ali and Desmons (2006) [22] developed a mathematical model, using the method step by step, to determine the thermal performances of the flat plate collector, see Fig. 22. The model can predict the temperature profile of all the components of the collector and of the air stream in the channel duct. Into the latter are introduced the offset rectangular plate fins, which increase the thermal heat transfer between the absorber plate and the fluid. The offset rectangular plate fins, mounted in a staggered pattern, are oriented parallel to the fluid flow and are soldered to the underside of the absorber plate. They are characterized by high heat transfer area per unit volume and generate the low pressure losses.

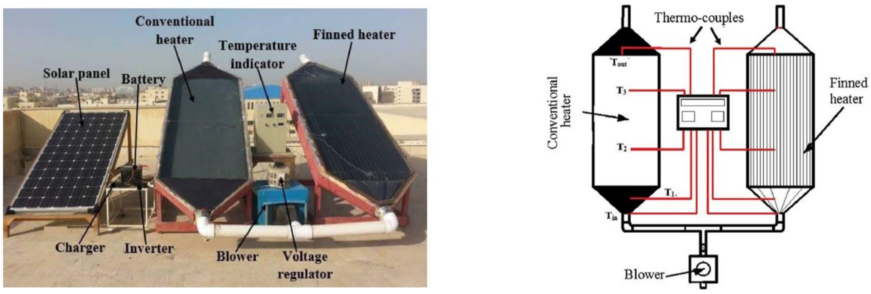

(a) **(b)**

Fig. 23. (a) Photo of the test-rig, (b) Schematic of the test-rig [23].

Kabeel et al. (2018) [23] communicated experimentally improving the performance of an entrance-modified single-pass Solar Air Heater (SAH) having nineteen longitudinal fins, see Fig. 23. Air Heater (SAH) having nineteen longitudinal fins. The longitudinal fins were used to increase the heat transfer area and to distribute the air flow uniformly in the channel. Experiments were conducted at three various heights of fins (3, 5, and 8 cm) to investigate the effect of the height. The entrance region was covered with glass cover instead of opaque or steel cover. In addition, guide blades were placed in the entry region to ensure good air distribution over the absorber surface. The experiments were performed at four various $\dot{m}$ varied between 0.013 kg/s and 0.04 kg/s. For each case of study, the performance of the modified SAH was compared with conventional one. The maximum daily efficiency of the ordinary finned SAH was 43.1% at 0.04 kg/s and 8 cm fins' height. Modifying the entrance region led to good enhancement in both output temperature and efficiency. For the modified finned SAH, the highest daily efficiency was 57% at 0.04 kg/s with fins' height of 8 cm. While for the conventional SAH, the highest daily efficiency was about 32 %.

(a) **(b)** **(c)** **(d)**

Fig. 24. A schematic illustration of the flat-plate solar air collector used in the test. (a) Schematic of the solar air collector, (b) The absorber plate, (c) The straight fins at the back of the absorber plate directly made by folding, (d) Thermal insulation at the back [24].

Deng et al. (2016) [24] used a simple dynamic characterization model of flat-plate solar collectors based on the piston flow concept to identify the collector characteristic parameters and to predict the dynamic thermal performance, see Fig. 24. The simple dynamic model was essentially the first-order finite difference solution of the ODE by dividing the collector into N equal segments along the flow direction. The model was compared to the numerical solution of ODE using the fourth-order

Runge-Kutta method and the improved TIM based on the closed-form integral solution. The results showed that the simple dynamic model predicts fairly well as the other two solution models except some special conditions such as sharply changed solar irradiance and collector inlet temperature.

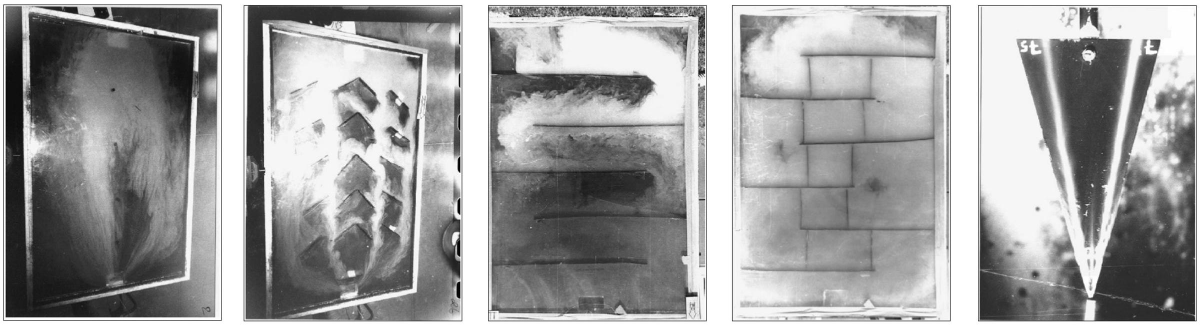

(a) **(b)** **(c)** **(d)** **(e)**

Fig. 25. Visualization of the air flow rate for collectors (a) without baffles, (b) with small baffles, (c) with transversal baffles, (d) with transversal and longitudinal baffles, (e) with Delta wing-shaped baffles [25].

Ben Slama (2007) [25] carried out experimental studies to visualize the air flow inside a flat-plate solar collector, using white smoke injected into the mobile air channel. This method shows the localization of the dead zones as well as the shape of vortices engendered by baffles. These baffles were placed in the 25 mm thick mobile air channel located between insulator and the absorber. Five different solar air channel designs, namely, channel without baffles, channel with small baffles, channel with transversal baffles, channel with transversal and longitudinal baffles, and channel with delta wing-shaped baffles, were visualized in that study, which are referred as cases A, B, C, D, and E, respectively, see Fig. 25. For the case A, the author observed that there is a direct passage of the air in the medium of the channel, from the inlet towards the outlet. In addition, there are many dead zones. For the case B, the dead zones were located downstream of the baffles. It was remarkable to observe that their extent is considerable. For the case C, the author observed the formation of a meandering flow. In this case, it was clear that the length of the trajectory is more than double that of the channel, thus increasing the air speed and the heat transfer. On the other hand, the size of the dead zones was considerable. For the case D, the efficiency was very much increased, and in the case E, the delta wings, as indicated by the author, have the characteristic to form two vortices on their extrados. This depends on their opening and incidence angles.

Baccoli et al. (2015) [26] presented a theoretical analysis of a collector augmented by a bottom booster reflector, see Fig. 26. An analytical model was developed and used to estimate the solar irradiation passing through the transparent cover of a flat collector, both with and without a bottom reflector. The analytical model was based on the anisotropic sky model and takes into account a finite length system with different angular configurations and reciprocal shading and reflections between reflector and collector. Computer simulations were carried out in order to find the optimum angles of the reflector with respect to the plane of the collector. Optimal inclinations of the collector and reflector for each month at 39° N latitude were identified.

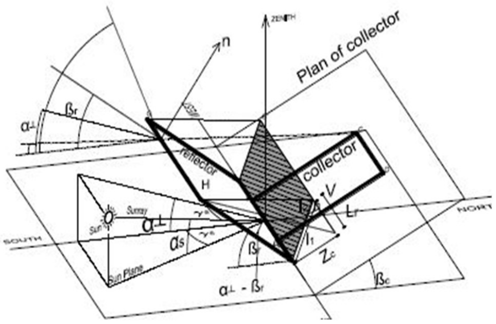

Fig. 26. A mathematical model of a solar collector augmented by a flat plate above reflector: optimum inclination of collector and reflector [26].

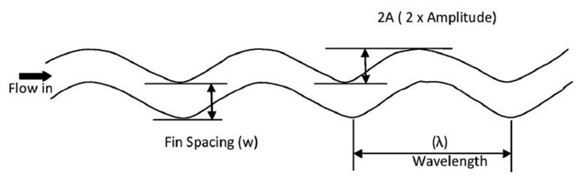

Fig. 27. Geometrical description and flow representation of a wavy fin [27].

Priyam and Chand (2018) [27] presented a theoretical study for computing the effects of amplitude and wavelength of the wavy fin on the thermal performance of a single pass flat plate solar air heater, see Fig. 27. A C++ program code with an iterative solution procedure was developed to solve the governing energy equations and to evaluate the mean temperatures of the collector. The effect of mass flow rate, amplitude and wavelength variation of the wavy fin on the thermal and thermohydraulic performance of present solar air heater was investigated. The results showed a great enhancement in the thermal and thermohydraulic performance with the modified solar air heater.

Manjunath et al. (2018) [28] presented the effect of sinusoidal profiled absorber plate on augmented heat transfer and corresponding thermo-hydraulic performance of solar air heater using three dimensional Computational Fluid Dynamics (CFD) simulation for the flow Reynolds number ranging between 4,000 and 24,000. The effect of variation of design parameters of corrugated absorber plate such as the non-dimensional wavelength and aspect ratio on the thermo-hydraulic performance was brought out, see Fig. 28. The aspect ratio was varied between 1.5 and 4.0 while the normalized wavelength was varied between 1.0 and 6.0. The study revealed that the presence of sinusoidal corrugations provides increased flow disturbances leading to considerable enhancement in heat transfer.

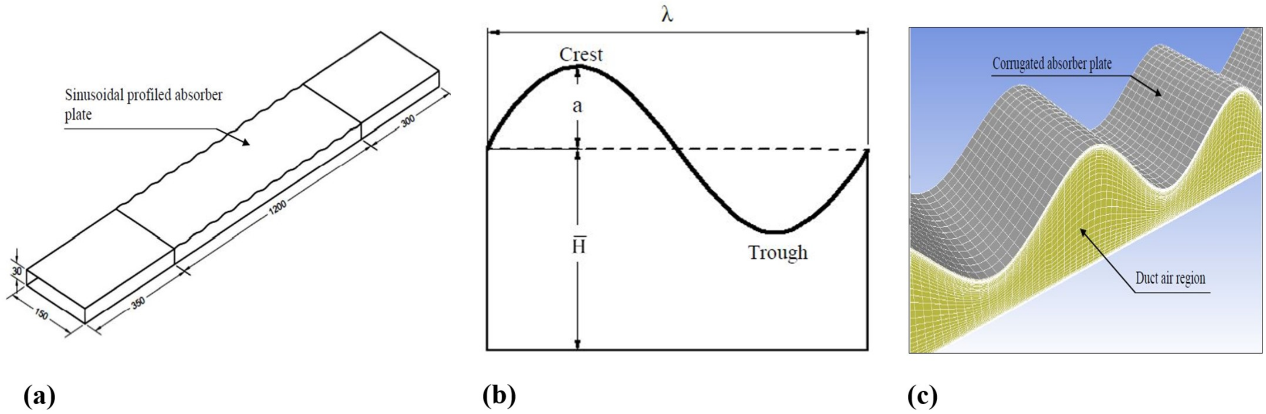

Fig. 28. (a) Geometric details of the computational domain of air duct fitted with sinusoidal profiled absorber plate, (b) Design parameters of sinusoidal corrugations on the absorber plate used in the analysis, (c) A close-up view of the mesh of a portion of air-duct and absorber plate [28].

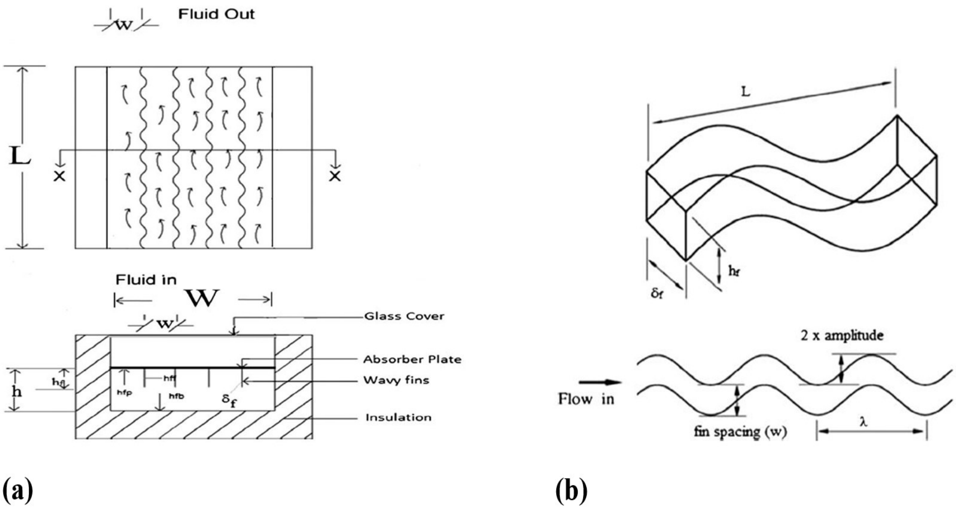

Fig. 29. (a) Solar air heater with wavy finned absorber, (b) Geometrical description and flow representation of a wavy fin [29].

Priyam and Chand (2016) [29] investigated analytically the performance analysis of a finned absorber solar air heater, see Fig. 29. The fluid channel is formed by two transversely positioned wavy fins attached on the absorber plate with bottom side thermally insulated and the top surface of absorber subjected to uniform heat flux. The expression for collector efficiency factor of such collector was developed. Effects of mass flow rates and fin spacings on the thermal performance were presented and the results were compared with plain solar air heater. The mathematical model provided reasonable predictions of the performance of wavy fin solar air heater and it can be useful in designing such types of solar air heater.

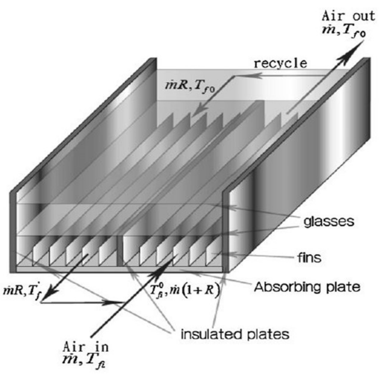

Fig. 30. Diagram of an upward-type internal-recycle flat-plate solar air heater with fins attached [30].

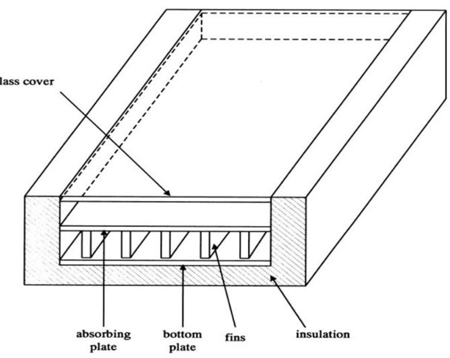

Fig. 31. Solar air heater with fins [31].

Yeh (2012) [30] investigated theoretically the effect of internal recycle on the collector efficiency in upward-type flat-plate solar air heaters attached with fins, see Fig. 30. The equations for predicting the outlet air temperature and the collector efficiency were derived from the energy balances on the absorbing plate and flow air. Considerable improvement in collector efficiency was obtainable if collector was attached with fins to extend the heat-transfer area, and if the operation was carried out with an internal recycle to increase the fluid velocity, leading to improved heat transfer coefficient. The enhancement in collector efficiency increased with increasing reflux ratio, especially for operating at lower air flow rate with higher inlet air temperature. The author found that more than 100 % of improvement in collector efficiency was obtained by recycling operation.

Yeh et al. (1998) [31] theoretically investigated the effect of collector aspect ratio on the collector efficiency of baffled solar air heaters, see Fig. 31. They concluded that either increasing the collector aspect ratio or providing fins attached with baffles on the collector, will improve the collector efficiency, However, increasing the collector aspect ratio or constructing the collector with fins and baffles not only increases the fixed charge but also increases the fan power and thereby leads to increased operating cost. Consequently, proper increase of the collector aspect ratio and proper installation of fins and baffles should be economically feasible in the design of a solar air heater.

Bekele et al. (2011) [32] carried out an experimental investigation to study the effect of delta-shaped obstacles mounted on the absorber surface of an air heater duct with an aspect ratio 6 : 1 resembling the conditions close to solar air heaters, see Fig. 32. Investigations were carried out over a wide range of Reynolds number (Re = 3400 - 27,600) and results were compared with those of a smooth duct under similar flow conditions to determine enhancement in heat transfer coefficient and friction factor. In general, they found that for all the relative height and any arrangement of obstacles, the enhancement of heat transfer is caused due to the increased turbulence and also due to the secondary flow of air produced along the obstacles, which carry the heated air away from the plate surface.

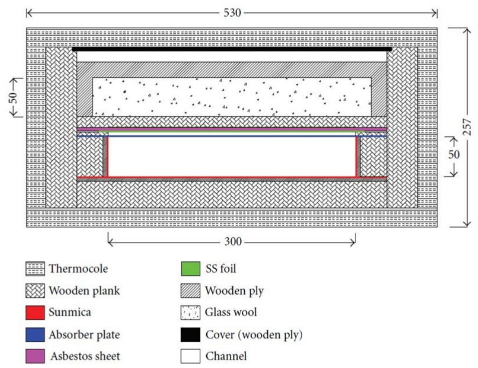

Fig. 32. Cross-sectional details of test section (Section X-X) [32].

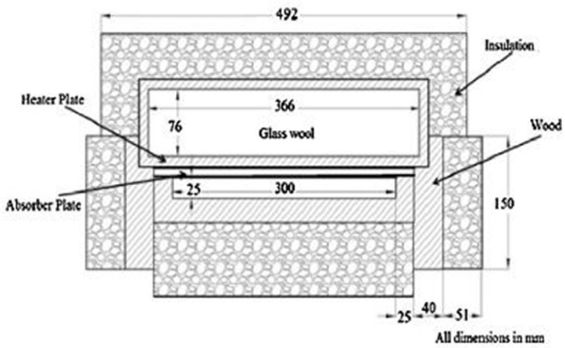

Fig. 33. Cross-sectional view of duct [33].

Alam et al. (2014) [33] experimentally investigated the effect of geometrical parameters of the V-shaped perforated blocks on heat transfer and flow characteristics of a rectangular duct of solar air heater, see Fig. 33. Extensive experimental data was collected on heat transfer and friction characteristics as function of geometrical parameters of these blocks, namely, relative height (e/H), open area ratio (b) and relative pitch ratio (P/e). They concluded that Nusselt number and friction factor are strongly depended on the open area ratio, relative blockage height and relative pitch ratio.

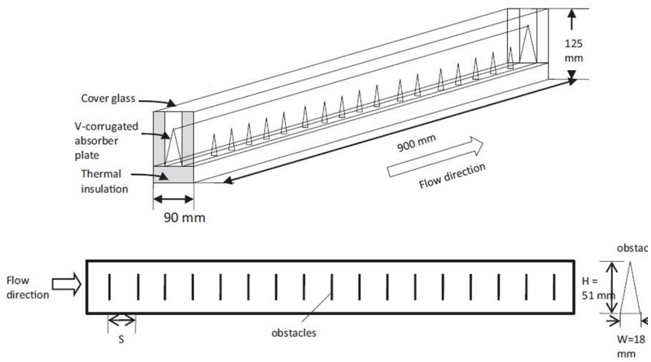

Fig. 34. Schematic of the solar collector model [34].

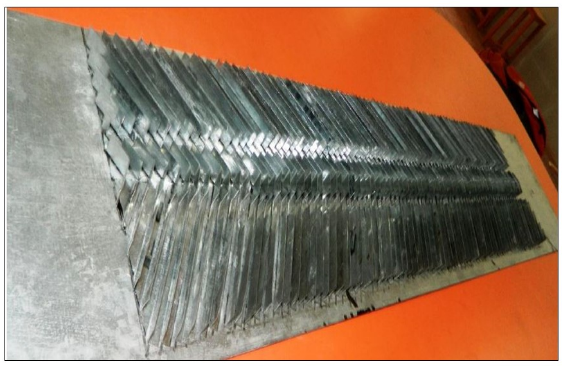

Fig. 35. Photographic view of discretized broken V-pattern baffle roughened plate [35].

Handoyo et al. (2016) [34] described the result of the numerical studies of obstacles' spacing inserted in a v-corrugated channel of a SAH, see Fig. 34. From numerical studies in a v-corrugated duct, they found that backflow between obstacles and high velocity in the gap between obstacles and absorber plate causes the flow became more turbulent and enhanced the convection heat transfer between the air and the absorber plate. Thus, when it is applied to SAH, it will improve its efficiency but increase the air pressure drop.

Kumar et al. (2016) [35] examined the augmentation in heat transfer and friction in a flow through solar air channel with discretized broken V-pattern baffle, see Fig. 35. The effect of relative baffle height, relative baffle gap width, relative baffle gap distance, relative baffle pitch and angle of attack on and was studied. By the use of the experimental data, correlations for heat transfer and friction characteristics were developed for solar air channel as function of system parameters of discretized broken V-pattern baffle.

Kumar et al. (2016) [36] experimentally studied the effect of angle of attack of the discrete V-pattern baffle on thermohydraulic performance of rectangular channel, see Fig. 36. The baffle wall was constantly heated and the other three walls of the channel were kept insulated. The experimentations were conducted to collect the data on Nusselt number and friction factor by varying the Reynolds number Re = 3000 - 21,000 and angle of attack from 30° to 70°, for the kept values of relative baffle height Hb/H = 0:50, relative pitch ratio Pb/H = 1:0, relative discrete width gw/Hb = 1:5 and relative discrete distance Dd/Lv = 0:67. The discrete V-pattern baffle shapes with angle of attack of 60° equivalent to flow Reynolds number of 3,000 yields the greatest thermohydraulic performance. Discrete V-pattern baffle has improved thermal performance as compared to other baffle shapes' rectangular channel.

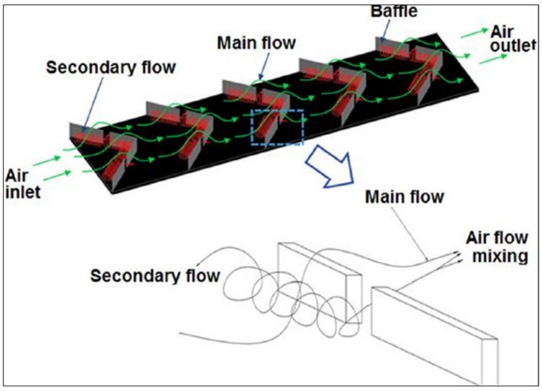

Fig. 36. Secondary stream pattern for discrete V-pattern baffle [36].

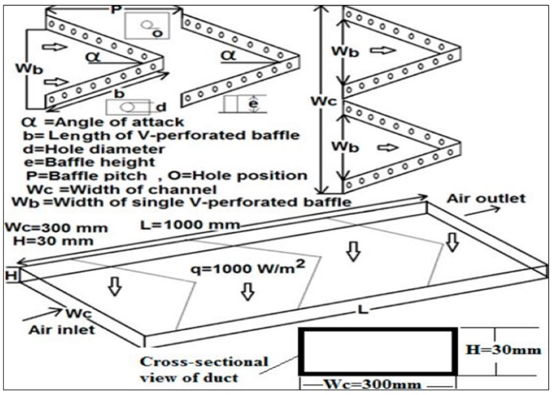

Fig. 37. Multi V-shaped perforated baffle shape [37].

Kumar and Kim (2016) [37] presented heat transfer and fluid flow characteristics in a solar air heater (SAH) channel with multi V-type perforated baffles, see Fig. 37. The flow passage has an aspect ratio of 10. The relative baffle height, relative pitch, relative baffle hole position, flow attack angle, and baffle open area ratio were 0.6, 8.0, 0.42, 60°, and 12%, respectively. The numerical results were in good agreement with the experimental data for the range considered in the study. Multi V-type perforated baffles were shown to have better thermal performance as compared to other baffle shapes in a rectangular passage. The overall thermal hydraulic performance showed the maximum value at the relative baffle width of 5.0.

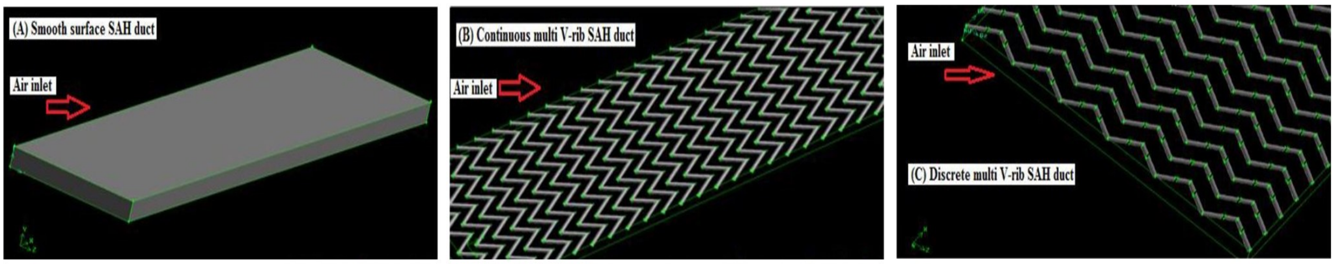

Fig. 38. Roughness elements: (a) Smooth SAH channel; (B) Continuous multi V-pattern rib SAH channel; (**c**) Discrete multi V-pattern rib SAH channel [38].

Kumar and Kim (2016) [38] reported the heat transfer and fluid flow characteristics in a rib-roughened SAH (solar air hea ter) channel, see Fig. 38. The artificial roughness of the rectangular channel was in the form of a thin circular wire in d iscrete multi V-pattern rib geometries. The effect of this geometry on heat transfer, fluid flow, and performance augment ation was investigated using the CFD technique. The thermo-hydraulic performance was found to be the best for the discrete width ratio of 1.0. A discrete multi V-pattern rib combined with dimple staggered ribs also had better overall thermal performance compared to other rib shapes.

Kumar et al. (2018) [39] experimental investigated the heat transfer and fluid flow characteristics in an air passage with different type of blockage arrangements as roughness elements employed over one wall, see Fig. 39. During the experimental examination air was passed through the test passage under a uniform wall heat flux of the heated wall plate. During the experimental study author found that the V-type perforated blockage provided better thermal hydraulic performance as compared with other type blockage air passage.

Hematian and Bakhtiari (2015) [40] designed and developed a solar collector, see Fig. 40. The experiments were performed in two convection modes and data were collected from 18-24 June 2011 throughout the day, in which atmospheric conditions were almost uniform. Thermal and efficiency analysis was carried out with the experiment data. Experimental results in natural and forced convection modes were evaluated and discussed. They concluded that the collector efficiency in forced convection was lower, but the low air temperature difference between inlet and outlet decreased its heat loss. They found that the average air speed in the forced convection was about 21% higher than the natural convection.

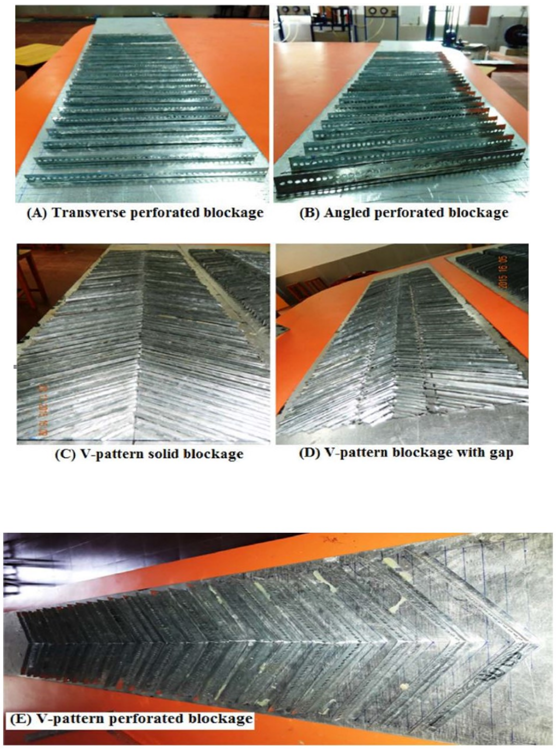

Fig. 39. Different type blockage roughness [39].

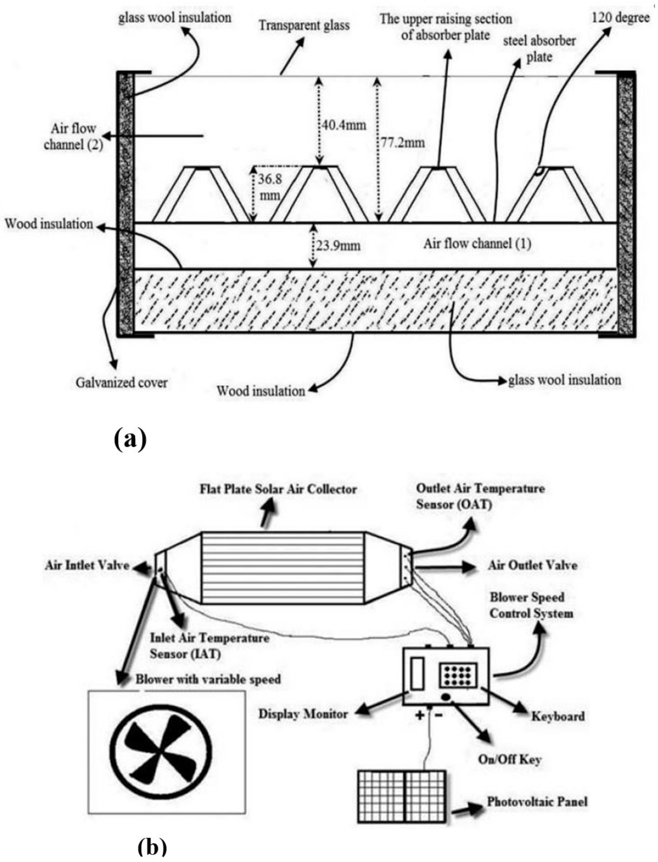

Fig. 40. (a) Schematic cross section of ASC, (b) Schematic view of system components [40].

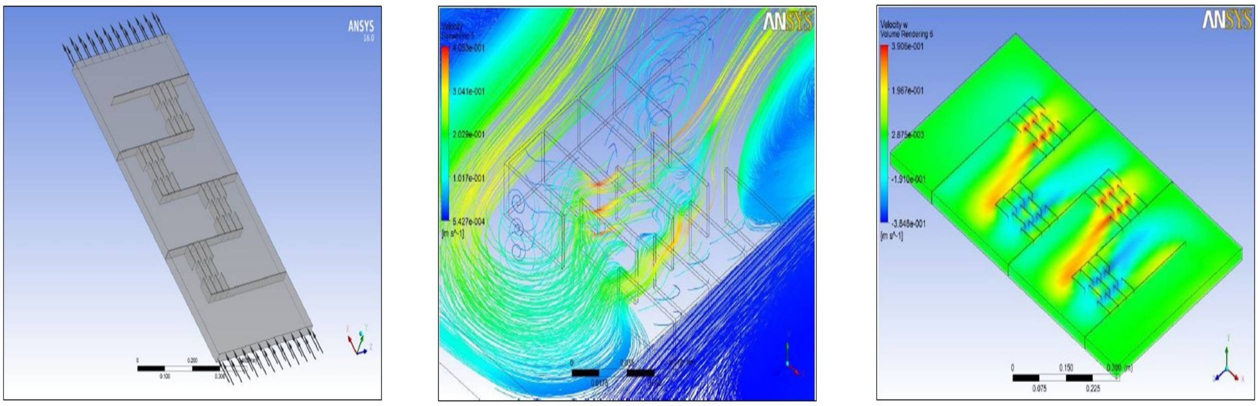

Fig. 41. (a) Sketch for the solar collector, Contour plots of (b) Streamlines, and (c) axial velocity field [41].

Amraoui and Aliane (2018) [41] show the design of air collector on which it is possible to act to improve the heat transfer between the absorber and the caloporting air and thus to favor the energetic efficiency while assuring a maximum increase of temperature, see Fig. 41. 3D model of the collector involving air inlet, the collector was modeled by ANSYS Workbench and the grid was created in ANSYS ICEM. The results were obtained by using ANSYS FLUENT and ANSYS CFX. The objective of this work was to compare theoretically and experimentally work done with the work done by using computational fluid dynamics (CFD) tool with respect to flow and temperature distribution inside the solar collector. The outlet temperature of air was compared with experimental results and there was a good agreement in between them.

3. Double and multi-pass flat plate solar air collectors

When SAHs were first developed, only a single air pass was employed to extract heat from the collector plate. However, recent research has proven that single-pass SAHs have low thermal performance because of high thermal losses to the environment. The air pass along the underside of the absorber plate extracts heat, and the air pass above the absorber plate regains a portion of the previously extracted heat; this causes an overall reduction in heat loss to the environment. The types of air pass configurations are the primary factor that affects the performance of a double-pass SAHs (Alam and Kim, 2017 [42]). In literature, numerous studies on various air pass configurations are reported, but only the relevant articles are cited here.

Sun et al. (2016) [43] presented a mathematical model based on numerical finite-difference approach under forced convection mode for the SAC. Airflow channel, absorber plate, glass cover, thermal insulation board and fan power were taken into consideration in this model and analyzed in detail, see Figs. 42 and 43. In order to verify the accuracy of this model, an indoor experimental system was built to study the performance of a double pass flow SAC. The effect of the inlet mass flow rate of the collector on the thermal performance was investigated under various environmental conditions. The outlet air temperature obtained from the theoretical and experimental studies were in reasonable agreement, which supports the validity of the theoretical model. The results were useful for analyzing and designing new SACs

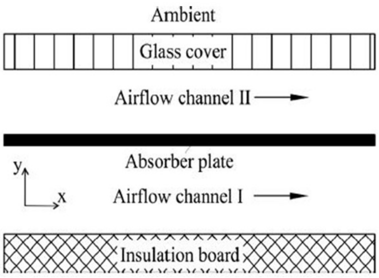

Fig. 42. Schematic of the solar collector model [43].

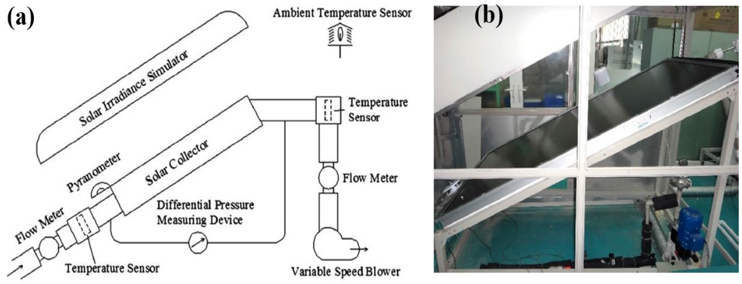

Fig. 43. (a) Schematic diagram, and (b) Photograph of the experimental setup [43].

Nowzari et al. (2015) [44] performed an experimental investigation on a solar air heater with different configurations, see Fig. 44. The configurations included testing the single- and double-pass solar collectors with normal and perforated covers and with wire mesh layers instead of an absorber plate. Design and analysis of experiment was used to develop a model for the tested solar air heater and IBM's Statistical Package for the Social Sciences software was used to analyze the model. Strong agreement was found between the results obtained from the theoretical and experimental investigations. Both methods suggested the same configuration for attaining the highest thermal efficiency from the system, i.e., a double-pass solar collector with a quarter-perforated cover with 3-cm hole-to-hole spacing and a mass flow rate of 0.032 kg/s.

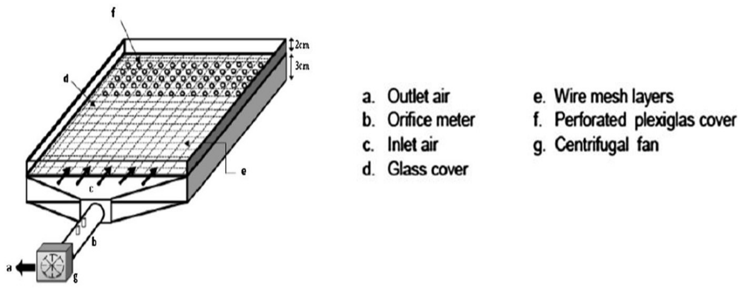

Fig. 44. Schematic assembly of the manufactured solar air heater [44].

Yeh and Ho (2011) [45] theoretically investigated the effect of internal-recycle operation on the collector efficiency in flat-plate solar air heaters, see Fig. 45. They found that considerable improvement in collector efficiency is obtainable if the operation is carried out with an internal recycle, where the desirable effect of increasing fluid velocity to decrease the heat transfer resistance compensates for the undesirable effect of decreasing the driving force (temperature difference) of heat transfer, due to the remixing effect at the inlet by recycle operation. The enhancement increased with increasing reflux ratio, especially for operating at lower air flow rate, as well as with higher solar radiation incident and inlet air temperature.

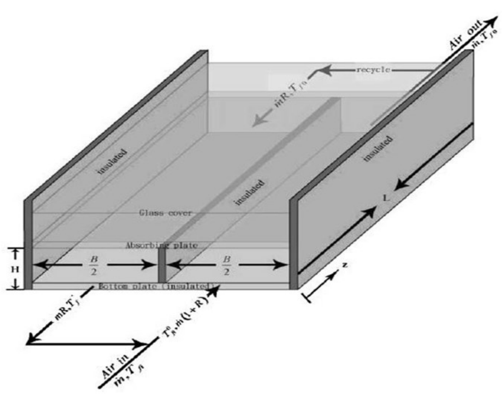

Fig. 45. Solar air collector with internal recycle [45].

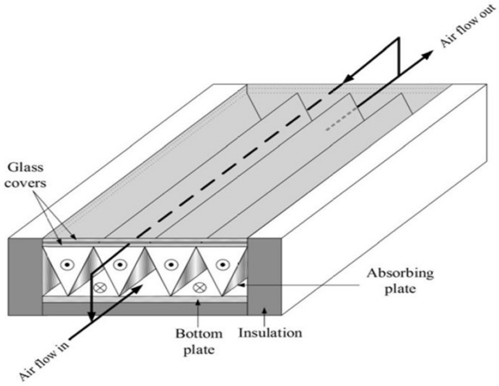

Fig. 46. Configuration of a recycling double-pass V-corrugated solar air collector [46].

Ho et al. (2017) [46] proposed a new design of recycling double-pass solar air collectors which incorporates a V-corrugated absorber to the conventional flat-plate device for increasing thermal efficiency, see Fig. 46. With the air flowing over and under the V-corrugated absorbing plate, the turbulence intensity as well as the convective heat transfer coefficient were enhanced. The theoretical predictions and experimental results were presented graphically and showed that both higher air mass flow rate and recycle ratio can lead to improvement of the collector performance as compared to that of the flat plate solar air collectors.

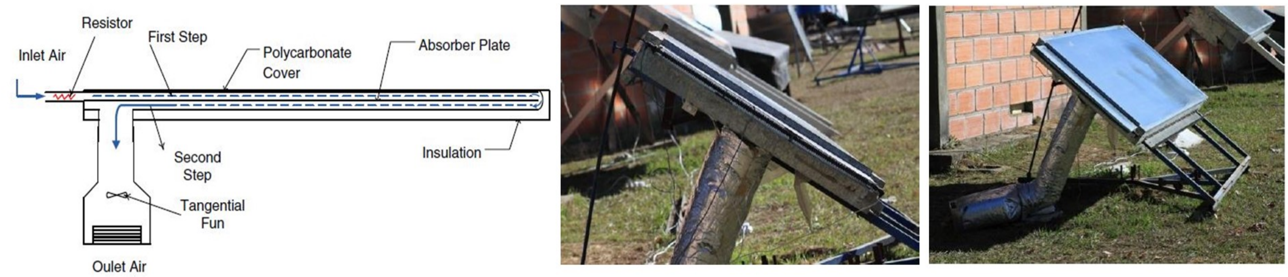

(a) **(b)** **(c)**

Fig. 47. (a) Scheme of the studied double-pass solar air collector. (b) Photo of the air inlet collector with the electric resistor, (c) Photo of the collector during the experience [47].

González et al. (2014) [47] showed the experimental study of the thermal efficiency of a counter-flow double-pass solar air heater and the theoretical thermal model developed to describe its thermal behavior, see Fig. 47. The prototype was designed and manufactured at INENCO, Universidad Nacional de Salta, Argentina, The useful collection area is 2 m2, and a channel height of 0.025 m. Experimental outdoor tests were carried out during a winter period, with maximum solar irradiance on the collector plane around 1050 W/m2. A semi-empirical thermal model was developed in order to simulate the air temperature at the collector outlet under different outdoor climatic conditions and air flow. Experimental results and the predictions of the theoretical model were found to be in good agreement.

Hassan et al. (2017) [48] presented the effect of using different absorber plate configurations on the performance of double pass SAH with two inlet ports, see Fig. 48. Moreover, the effect of using different air flow percentages through the inlet ports was studied for each studied configuration. Four absorber plate configurations were considered; (i) flat plate (ii) pin finned, (iii) corrugated finned, and (iv) corrugated-perforated finned. Moreover, four percentages of the inlet air were considered: (i) 0 % of the air flows through the upper inlet port and 100 % through the lower inlet port (0 % Up), (ii) 33.3 % of the air flows through the upper inlet port and the remainder through the lower inlet port (33.3 % Up), (iii) 66.7 % of the air flows through the upper inlet port and the remainder through the lower inlet port (66.7 Up), and (iv) 100 % of air flows through the upper inlet port (100 % Up). The measurements were carried out during the day using the solar flux and at night using a solar simulator.

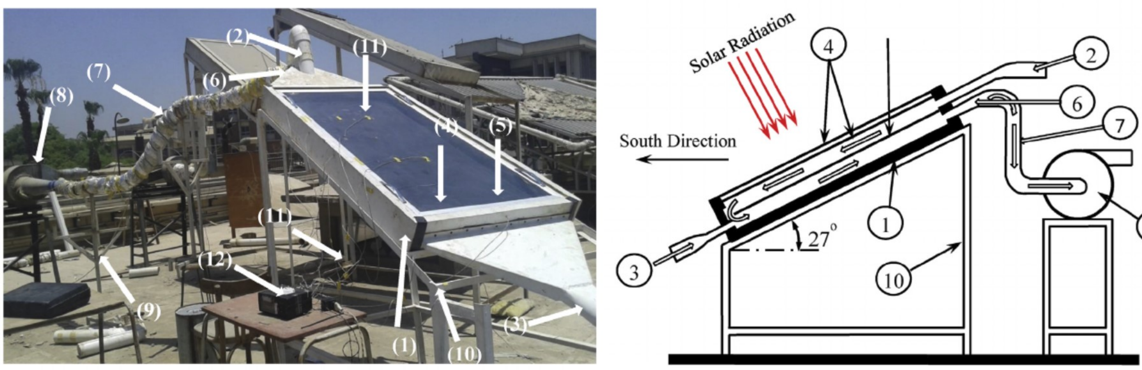

Fig. 48. The experimental setup. Wooden frame (1), Upper inlet port (2), Lower inlet port (3), Glass cover (4), Absorber plate (5), Outlet port (6), Insulated tube (7), Blower (8), Tube stand (9), Metal stand (10), thermocouples (11), Acquisition center (12) [48].

Ramani et al. (2010) [49] presented theoretical and experimental analysis of double pass solar air collector with and without porous material. A mathematical model was developed based on volumetric heat transfer coefficient. Effects of various parameters on the thermal performance and pressure drop characteristics were discussed. Comparison of results reveals that the thermal efficiency of double pass solar air collector with porous absorbing material was 20 - 25 % and 30 - 35 % higher than that of double pass solar air collector without porous absorbing material and single pass collector respectively.

Fudholi et al. (2013) [50] conducted the performance and cost benefit analysis of double-pass solar collector with and without fins, see Fig. 50. The theoretical model using steady state analysis was developed and compared with the experimental results. The performance curves of the double-pass solar collector with and without fins, which included the effects of mass flow rate and solar intensity on the thermal efficiency of the solar collector, were obtained. Results indicated that the thermal efficiency is proportional to the solar intensity at a specific mass flow rate. The thermal efficiency increased by 9 % at a solar intensity of 425 - 790 W/m2 and mass flow rate of 0.09 kg/s.

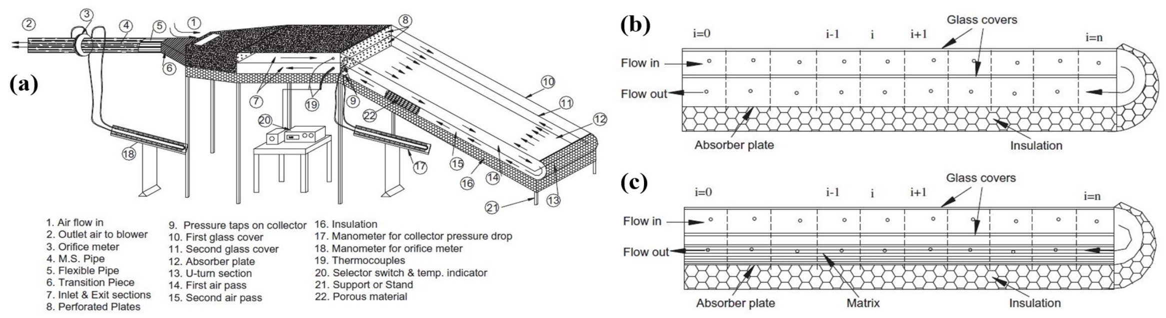

Fig. 49. (a) Schematic diagram of experimental set up. Double pass arrangement: (b) without porous material, (c) with porous material [49].

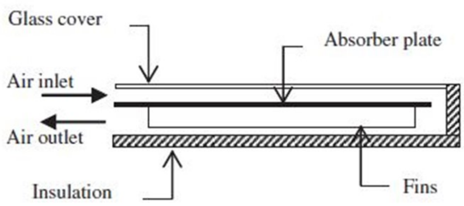

Fig. 50. Schematic of a double-pass solar collector with fins absorber in the second channel [50].

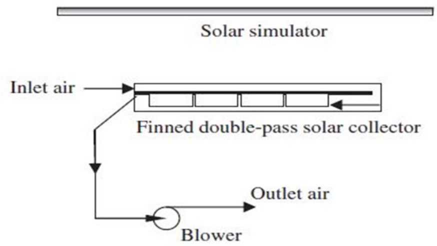

Fig. 51. Test facility of solar collector. [51].

Fudholi et al. (2013) [51] developed steady state energy balance equations for the finned double-pass solar collector, see Fig. 51. These equations were solved using the matrix inversion method. The predicted results were in agreement with the results obtained from the experiments. The predictions and experiments were observed at the mass flow rate ranging between 0.03 kg/s and 0.1 kg/s, and solar radiation ranging between 400 W/m2 and 800 W/m2. The effects of mass flow rates and solar radiation levels on energy efficiency, exergy efficiency and the improvement potential were observed.

Lertsatitthanakorn et al. (2008) [52] developed and tested a double-pass TE solar air collector, see Fig. 52. The TE solar collector was composed of transparent glass, air gap, an absorber plate, thermoelectric modules and rectangular fin heat sink. The incident solar radiation heats up the absorber plate so that a temperature difference was created between the thermoelectric modules that generates a direct current. The proposed theoretical model may be used for predicting the output power of the TE modules with reasonable accuracy given temperature difference conditions.

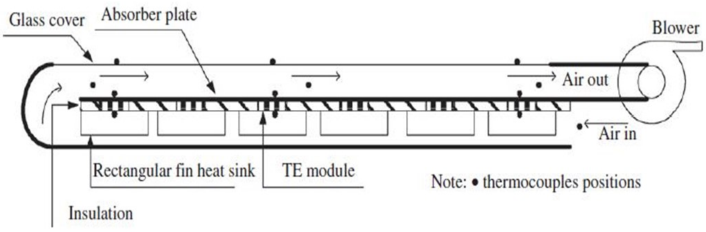

Fig. 52. A schematic diagram of the TE solar air collector [52].

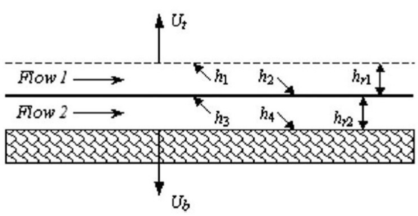

Fig. 53. Details of the heat transfer coefficients inside the solar collector [53].

Hernández and Quiñonez (2013) [53] presented the development of two analytical models that describe the thermal behaviour of solar air heaters of double-parallel flow and double-pass counter flow. Based on the local energy balances, algebraic expressions for the efficiency factor F' and the overall heat loss coefficient, UL, as well as air temperature distributions along the collectors were obtained, see Fig. 53. In addition, the expressions of the mean temperatures of the two air streams and of the absorber plate were determined. The model corresponding to the solar collector with double-parallel flow predicts that the mass flow of air flowing between the absorber plate and the transparent cover was greater than the mass flow circulating through the other channel. The model corresponding to the solar collector of double-pass counter flow indicated that increasing the airflow proportionally increases the percentage temperature rise in the inlet channel. The analytical expressions developed were valuable tools that can be included in computational codes for the design and thermal analysis of solar air heating facilities or to improve current facilities. The paper included a graphic to estimate the heat transfer coefficients involved in energy balances.

Aldabbagh et al. (2010) [54] experimentally investigated the thermal performances of single and double pass solar air heaters with steel wire mesh layers are used instead of a flat absorber plate, see Fig. 54. The effects of mass flow rate of air on the outlet temperature and thermal efficiency were studied. The results indicate that the efficiency increases with increasing the mass flow rate for the range of the flow rate used in this work between 0.012 and 0.038 kg/s. For the same flow rate, the efficiency of the double pass was found to be higher than the single pass by 34 - 45 %. Comparison of the results of a packed bed collector with those of a conventional collector showed a substantial enhancement in the thermal efficiency.

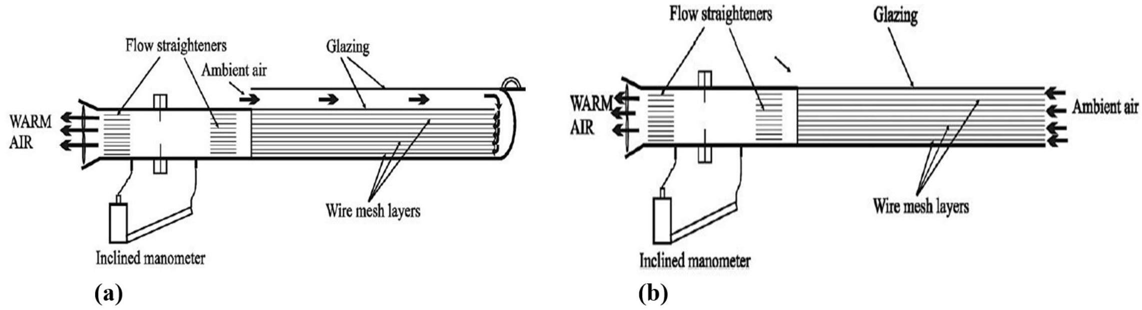

Fig. 54. (a) Side view of the double pass SAH and (b) side view of the single pass SAH [54].

Sopian et al. (2009) [55] developed a theoretical model for the double-pass solar collector, see Fig. 55. An experimental setup was designed and constructed. The porous media was arranged in different porosities to increase heat transfer, area density and the total heat transfer rate. Comparisons of the theoretical and the experimental results were conducted. Such comparisons included the outlet temperatures and thermal efficiencies of the solar collector for various design and operating conditions. The relationships included the effect of changes in upper and lower channel depth on the thermal efficiency with and without porous media. Moreover, the effects of mass flow rate, solar radiation, and temperature rises on the thermal efficiency of the double-pass solar collector have been studied. The study concluded that the presence of porous media in the second channel increases the outlet temperature, therefore increases the thermal efficiency of the systems.

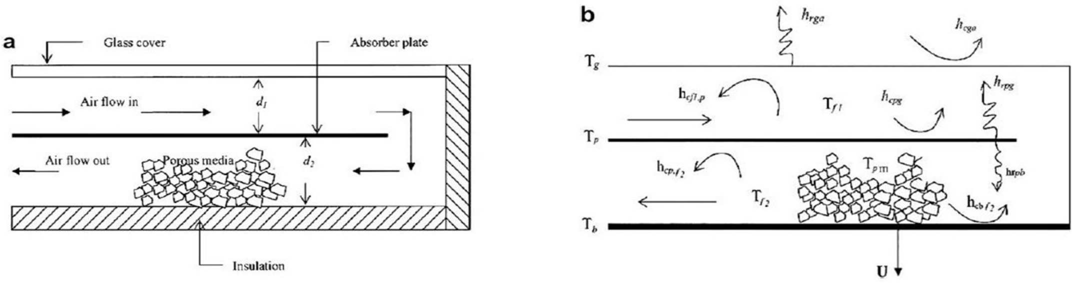

Fig. 55. (a) Schematic of the double-pass solar collector with porous media. (b) Schematic of heat transfer coefficients in the double-pass solar collector. [55].

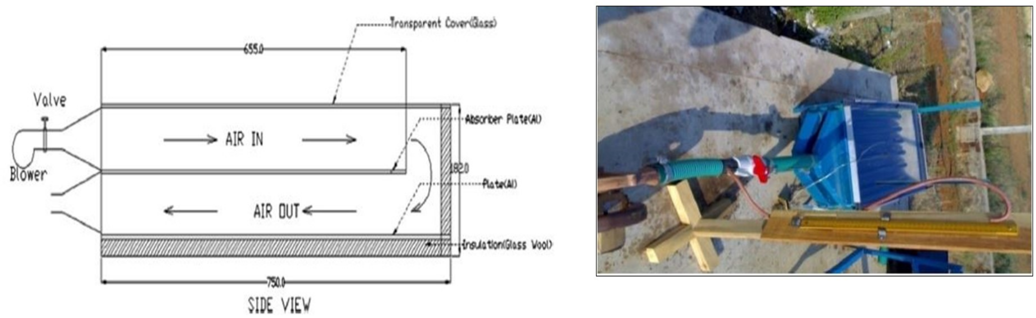

Fig. 56. Schematic diagram and photograph for double pass solar air heater [56].

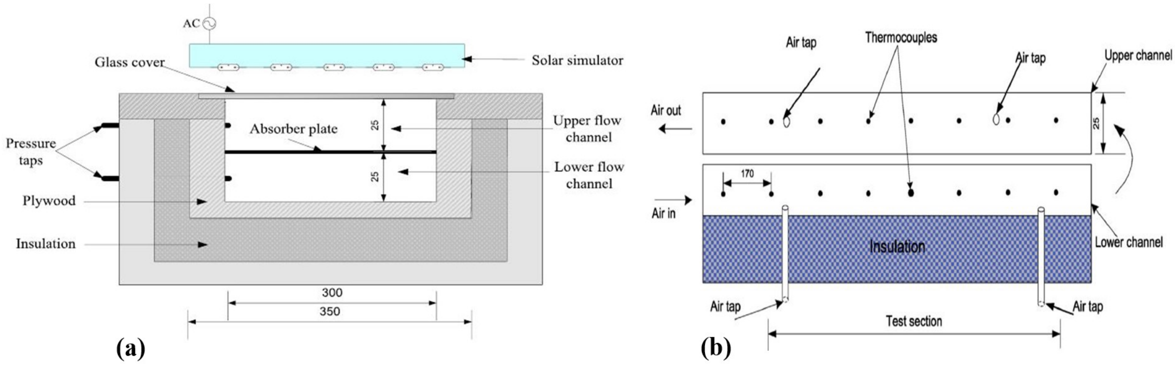

Fig. 57. (a) Cross section of the duct, (b) Location of thermocouples and air taps in air duct. [57].

Krishnananth and Murugavel (2013) [56] fabricated and integrated a double pass solar air heater with thermal storage system, see Fig. 56. Paraffin wax was used as a thermal storage medium. The performance of this heater was studied for different configurations. The solar heater integrated with thermal storage delivered comparatively high temperature. The efficiency of the air heater integrated with thermal storage was also higher than the air heater without thermal storage system. The study concluded that the presence of the thermal storage medium at the absorber plate is the best configuration.

Ravi and Saini (2016) [57] conducted an experimental analysis to study the effect of roughness parameters on thermohydraulic performance of double pass duct having discrete multi V shaped and staggered rib, see Fig. 57. The effect of the increase in relative staggered rib size (r/e) ratio and Reynolds number (Re) on friction factor and Nusselt number was evaluated in order to examine the thermal and thermohydraulic characteristics of the duct to figure out the advantages of the selected roughness pattern. Based on the study, heat transfer and pressure drop in single and double pass mode were estimated at range of ribs and performance parameters and results were compared with smooth ducts under same operating conditions. The author found that the roughness geometry used on each side of the plate in double pass mode enhances both frictional losses as well as heat dissipation rate.

Ho et al. (2013) [58] experimentally and theoretically investigated the device performance of the new design of wire mesh packed double-pass solar air heaters with attaching wire mesh under external recycle, see Fig. 58. The improvement of device performance of wire mesh packed solar air heaters with different flow patterns was represented graphically and compared, including the single-pass, flat-plate double-pass with recycle and wire mesh packed double-pass with recycle. Heat transfer improvement was considerably obtained by employing such a recyclic double-pass with wire mesh packed, instead of using the flat-plate single-pass operation. The wire mesh packed double-pass device introduced in this study was proposed for aiming to strengthen the convective heat transfer coefficient for air flowing through the wire mesh packed bed, and to determine the optimal design on an economic consideration in terms of both heat transfer efficiency improvement and power consumption increment. The effect of recycle ratio on the heat transfer efficiency enhancement as well as the power consumption increment was also delineated.

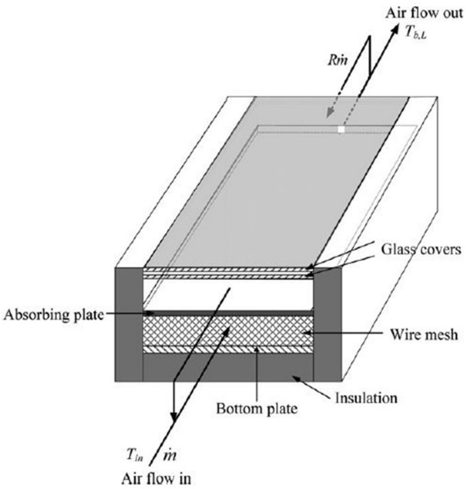

Fig. 58. A schematic drawing of a wire mesh packed double-pass solar air heater [58].

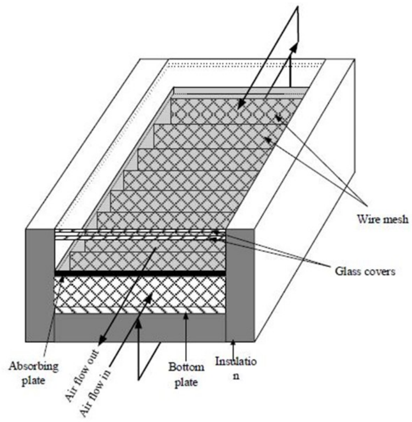

Fig. 59. Configuration of a double-pass solar air heater with recycle [59].

Ho et al. (2015) [59] developed analytically and experimentally the collector efficiency improvement in recycling double-pass solar air heaters with wire mesh packed, see Fig. 59. The comparisons of double-pass configurations with and without attaching wire mesh were made to investigate the device performance improvement. Consequently, applications of the recycle effect with wire mesh attachment for operating double-pass device are technically and economically feasible.

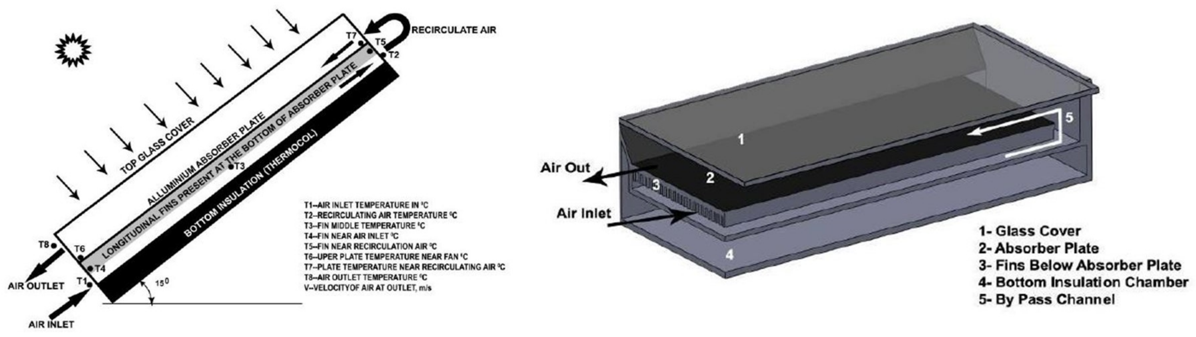

(a) **(b)**

Fig. 60. (a) Schematic diagram and (b) Sectional view of a DPSAH with bottom extended surface [60].

Pramanik et al. (2017) [60] prepared a model of solar air heater with selective absorber coating with longitudinal fins at the bottom of absorber to produce hot gases by consuming solar energy in day time, see Fig. 60. Its output temperature increases up to acceptable values as per our local atmospheric conditions. Consequently, applications of such type of solar air heaters can be used as a solar dryer for many agricultural requirements through the year in our country.

Dhiman et al. (2012) [61] theoretically and experimentally investigated the counter and parallel flow packed bed solar air heaters, see Fig. 61. Analytical model for these air heaters was presented. The effect of air mass flow rates and bed porosity on the thermal and thermohydraulic efficiencies of the counter and parallel flow packed bed solar air heaters were investigated. The results showed that the thermal efficiency of the counter flow packed bed solar air heater is 11 - 17 % more compared to the parallel flow packed bed solar air heater whereas, parallel flow system achieved a 10 % higher thermohydraulic efficiency when air steadily flowed at differential mass rates in its upper and lower ducts compared to the counter flow system.

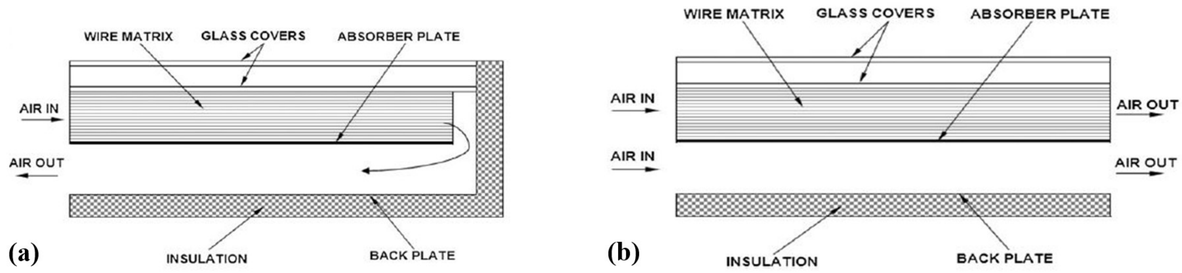

Fig. 61. Schematic diagram of (a) CFPBSAH and (b) PFPBSAH [61].

Singh and Dhiman (2015) [62] developed and analyzed two different models of double pass packed bed solar air heater under external recycle for the thermal and thermo-hydraulic performance improvement, see Fig. 62. The maximum thermal efficiency of Model-I was found to be about 79 %, while, for Model-II, it was found to be about 81 %. The thermal performance of the collectors increases with increasing recycle ratio and air mass flow rate. They obtained that the varying channel depth of the first channel as well as the single air pass has significant effect on the performance of these solar air collector models.

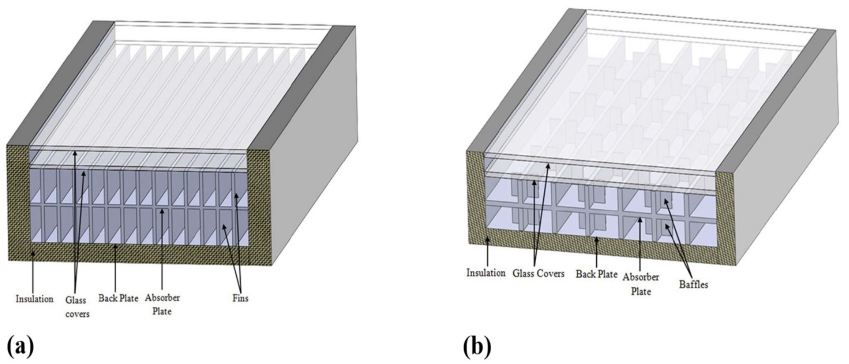

Fig. 62. Schematic diagram of double pass solar air heater with (a) fins and (b) fins with baffles [62].

Orbegoso et al. (2017) [63] numerically characterized the thermal behaviour of three configurations of solar air heating collectors in order to determine which demonstrated the best thermal performance under several controlled operating conditions. For this purpose, a computational fluid dynamics model was developed to describe the simultaneous convective and radiative heat transfer phenomena under several operation conditions. The constructed computational fluid dynamics model was firstly validated through comparison with the data measurements of a one-step solar air heating collector. They then simulated two further three step solar air heating collectors in order to identify which demonstrated the best thermal performance in terms of outlet air temperature and thermal efficiency. The numerical results showed that under the same solar irradiation area of exposition and operating conditions, the three-step solar air heating collector with the collector plate mounted between the second and third channels was 67 % more thermally efficient compared to the one-step solar air heating collector.

Kareem et al. (2016) [64] presented the performance of a new solar air heating collector of multi-pass mode. The solar air heating system was theoretically modelled by applying energy balance expressions to reflect the network of convection and radiation heat flows. The performance efficiency of the system collector was evaluated as 59.96 % under forced convective mode. Sensible thermal mass improved the performance of the system by 9.37 % when the maximum daily system inlet air velocity and environmental temperature were 0.63 ms-1 and 33.77° C, respectively.

Kareem et al. (2017) [65] conducted an experimental study of MPSAHC system under transient state in the open field of solar research site, Universiti Teknologi PETRONAS. The hot air delivered by the MPSAHC system attained 70.18 °C at the midday while the air generated by single pass, double pass and ambient temperature were 48.53 °C, 57.75 °C and 36.64 °C, respectively. The system achieved a maximum thermal collector efficiency of 72.59 % in this investigation. The daily average collector efficiency of 36.38 % was accomplished while the exergy efficiency ranged between 83 % and 67 % were recorded when the optimum air mass flow rate of 0.016 kgs-1 was applied. Sensible energy stored in the porous media has extended the thermal delivery of the system to the off-sun period.

4. Solar air collector applications

Solar air collectors have been used in a variety of applications. Selected works concerning these applications are reviewed in this section. Chen and Liu (2004) [66] studied the heat transfer and air flow in a composite-wall solar-collector system with a porous absorber, see Fig. 63. The unsteady numerical simulation was conducted to analyze the performance of heat transfer and air flow in the composite wall. The excess heat was stored in the porous absorber by the incident solar radiation, which leads to a temperature gradient in the porous layer, so that the absorber can work as a good thermal insulator when sunlight is not available. The influences of the particle size and the porosity of the porous absorber on the air temperature in the heated room were significant. The results showed that all these factors should be taken into account for a better design of the passive solar-heating system.

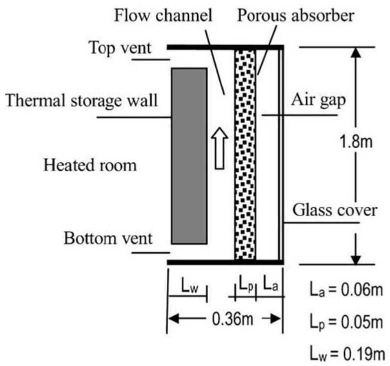

Fig. 63. Schematic of a composite wall solar collector with a porous absorber [66].

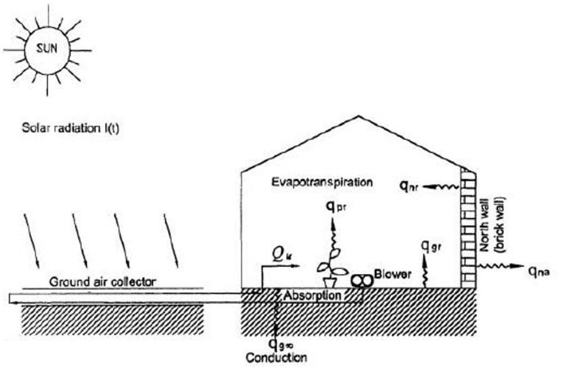

Fig. 64. Cross-sectional view of experimental greenhouse with north wall and GAC showing various heat fluxes [67].

Jain and Tiwari (2003) [67] devised a mathematical model to study the thermal behavior of a greenhouse while heating with a ground air collector (GAC), see Fig. 64. A computer program based on MatLab software was used to predict the plant and room temperatures as a function of various design parameters of the ground air collector. Extensive experiments were conducted during December 2000 to March 2001for an even span greenhouse of effective floor area of 24 m2 with a GAC and having a brick north wall. A parametric study involved the area of the GAC, mass flow rate and heat capacity. The predicted plant and room temperatures showed fair agreement with the experimental values.

Hatami and Bahadorinejad (2008) [68] studied a vertical flat-plate solar air heater, see Fig. 65. There were six case studies and it was shown that case study 6 has the highest thermal efficiency (air heater with 3 channels). New relations were proposed to evaluate natural convection heat transfer coefficient in air heater channels and enclosures.

Yang et al. (2014) [69] optimized by numerical modeling the design of a solar air heater with offset strip fins, see Fig. 66. A series of experiments based on ASHRAE Standard 93 - 2003 was conducted to test the detailed thermal performance of the heater in the light of time constant, thermal efficiency, incident angle modifier and the synthetical resistance coefficient. The work would be useful for developing energy efficient and cost effective solar air heaters.

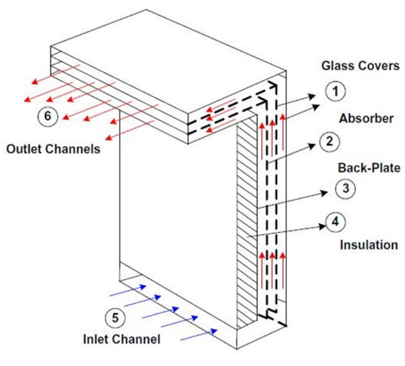

Fig. 65. Description of various parts of considered solar air heater [68].

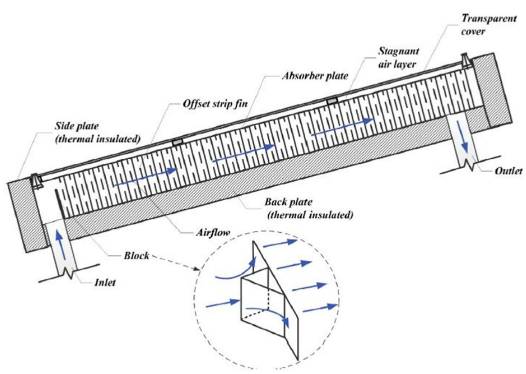

Fig. 66. Schematic view of the solar air collector with offset strip fin attached [69].

Kabeel (2007) [70] proposed a solar powered air conditioning system using liquid desiccant, see Fig. 67. A solar air heater containing a porous material was used for regeneration purpose in the proposed system. The honeycomb desiccant rotary wheel was constructed from iron wire and clothes layer impregnated with calcium chloride solution, in honeycomb form, was utilized for the regeneration and absorption processes. The effect of airflow rate and solar radiation intensity on the system regeneration and absorption processes were studied. The obtained results showed that the system is highly effective in the regeneration process.

Jain and Jain (2007) [71] presented a transient analytical model for an inclined multi-pass solar air heater with in-built thermal storage and attached with the deep-bed dryer, see Fig. 68. The performance of a solar air heater was evaluated for drying the paddy crop in a deep bed by using an appropriate deep-bed drying model. A parametric study was done for a day of the month of October for the climatic condition of Delhi (India). The effect of change in the tilt angle, length and breadth of a collector and mass flow rate on the temperature of grain were studied. The rate of moisture evaporation and humidity of the drying air were analyzed with the drying time for different depth of the grain bed. They observed that the bed moisture content decreases with the time of the day. The humidity of the air and the drying rate increased with the increase in the depth of drying bed.

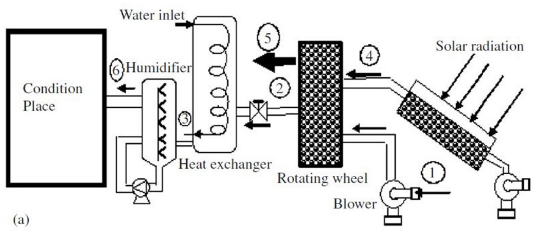

Fig. 67. Schematic of the proposed system [70].

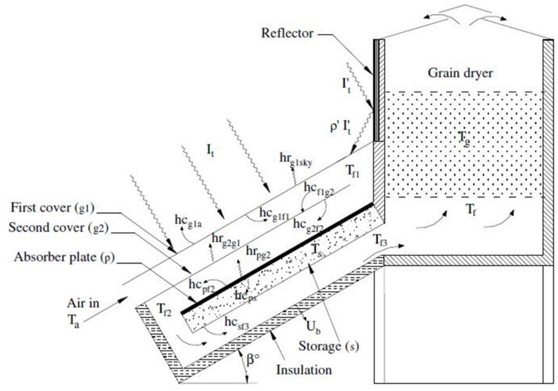

Fig. 68. Inclined multi-pass air heater with in-built thermal storage attached with deep-bed drying system [71].

Madhlopa et al. (2002) [72] designed a solar air heater, comprising two absorber systems in a single flat-plate collector, on the principles of psychrometry, see Fig. 69. The heater was integrated to a drying chamber for food dehydration. This collector design offered flexibility in manual adjustment of the thermal characteristics of the solar dryer. The performance of the dryer was evaluated by drying fresh samples of mango. The air heater converted up to 21.3 % of solar radiation to thermal power, and raised the temperature of the drying air from about 31.7 °C to 40.1 °C around noon. The dryer reduced the MC of sliced fresh mangoes from about 85 % (w/w) to 13 % (w/w) on wet basis, and retained 74 % of ascorbic acid. They found that the dryer was suitable for preservation of mangoes and other fresh foods.

Bennamoun and Belhamri (2003) [73] studied a simple efficient and inexpensive solar batch dryer for agriculture products, see Fig. 70. During periods of low sunshine a heater was used. The establishment of heat and mass balances leaded to two sets of differential equations completed by an empirical model, which represents the drying kinetics. Onion was chosen as the dried product because of its swift deterioration property. The shrinking effect was taken into consideration. The results showed that drying is affected by the surface of the collector, the air temperature and the product characteristics. Significant improvements were registered in the results, after the heater is added.

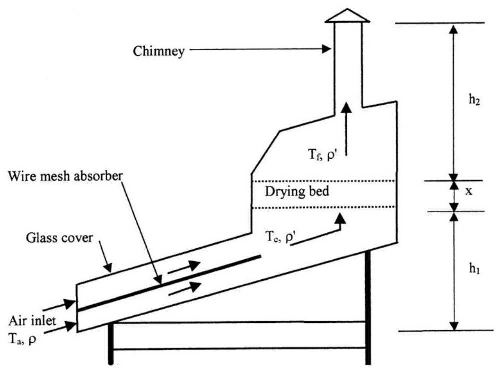

Fig. 69. Cross-section of solar dryer showing collector, drying chamber and chimney [72].

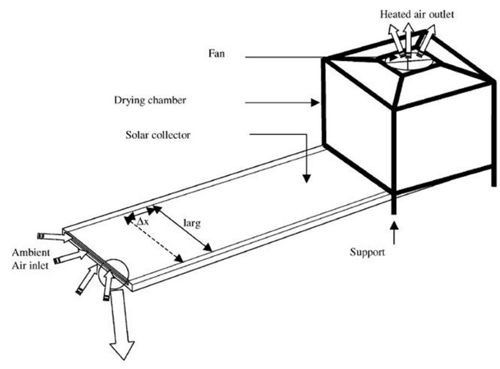

Fig. 70. Diagram of a solar batch dryer [73].

Janjai et al. (2008) [74] presented experimental performance of solar drying of rosella flower and chili using roof-integrated solar dryer and also presented modelling of the roof-integrated solar dryer for drying of chili, see Fig. 71. Field-level tests for deep bed drying of rosella flower and chili demonstrated that drying in the roof-integrated solar dryer results in significant reduction in drying time compared to the traditional sun drying method and the dry product is a quality dry product compared to the quality products in the markets. The payback period of the roof-integrated solar dryer was about 5 years. Two sets of equations were developed to simulate the performance of the roof-integrated solar dryer for drying herbs and spices using hot air from roof-integrated solar collectors. The first set of equations was solved implicitly and the second set of equations was solved explicitly using finite difference technique. The simulated air temperatures at the collector outlet agreed well with the observed air temperatures. Good agreement was also found between experimental and simulated moisture contents.

Kareem et al. (2016) [75] reported a study on the performance of a forced convective multi-pass solar air heating collector (MPSAHC) system assisted with granite as a sensible energy storing matrix, see Fig. 72. Experimental drying of Roselle was carried out in August 2015 at Solar Energy Research Site of Universiti Teknologi PETRONAS, Malaysia (4.385693o N and 100.979203 S). The investigation was conducted under the daily average relative humidity, solar irradiance, ambient temperature and wind speed of 64.5 %, 635.49 Wm-2, 32.24 °C, and 0.81 ms-1, respectively. An average drying rate of 33.57 g.(kg.m2.h)-1 was achieved while the system optical efficiency, collector efficiency, drying efficiency and moisture pickup efficiency of 70.53 %, 64.08 %, 36.22 % and 66.95 % were obtained, respectively. MPSAHC dryer was 21 h faster with fair color retention when compared to open sun drying approach (OSDA) that was conducted together under the same weather condition. Techno economic analysis reflected a payback 28 period of 2.14 years. However, drying efficiency could be improved if the inlet air humidity can be controlled to favor drying operation.

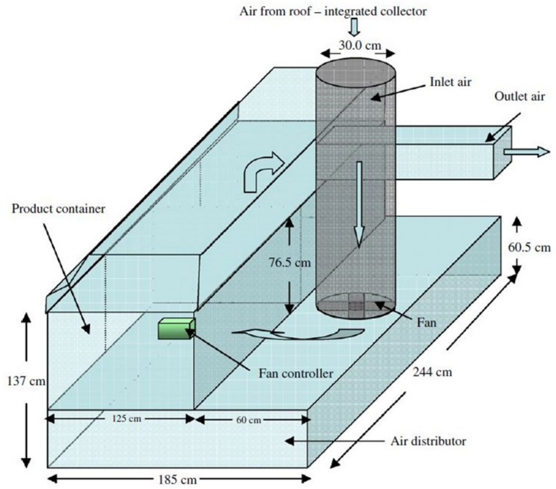

Fig. 71. The drying bin [74].

Fig. 72. Drying cabinet of 282 the MPSAHC system [75].

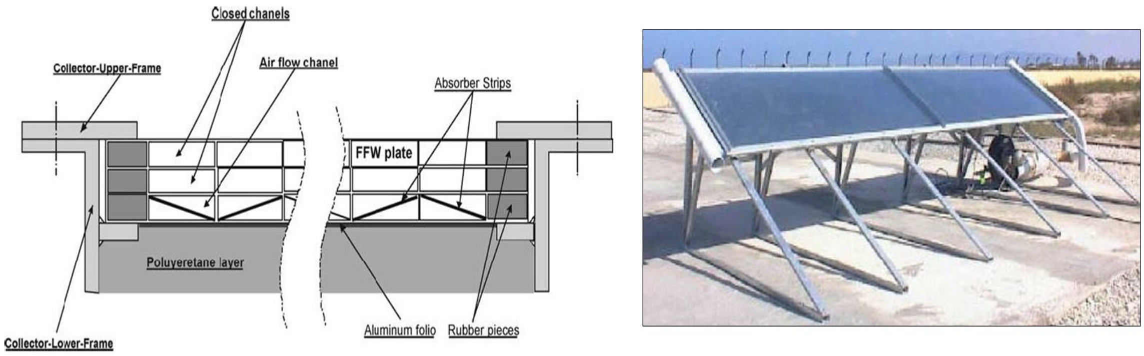

Fig. 73. (a) Cross-section of the collector, (b) Photo of the collector prototype installed on the INRST outdoor test setup [76].

Ben-Amara et al. (2005) [76] experimentally studied the efficiency of a new-design plate collector used to heat air in a new desalination humidification-dehumidification process, see Fig. 76. The effect of different parameters, namely: the solar radiation intensity, the wind velocity, the ambient temperature, the air mass flow rate, the inlet air humidity and temperature, on the collector thermal efficiency was investigated. The collector was characterized under the different experimental conditions. In addition, endurance-test on the collector prototype showed that this type of polycarbonate plate collector could not be used without a blower that ensures an air circulation in the chambers of the collector.

Moss et al. (2017) [77] presented a method for choosing the optimum channel hydraulic diameter subject to geometric similarity and pumping power constraints; this is an important preliminary design choice for any solar collector designer. The choice of pumping power was also illustrated in terms of relative energy source costs. Both microchannel and serpentine tube systems have an optimum passage diameter, albeit for different reasons. Double-pass and flooded panel designs were considered as special microchannel cases. To maintain efficiency, the pumping power per unit area must rise as the passage length increases. Beyond the optimum pumping power the rise in operating cost outweighs the increase in collector efficiency.

Karim and Hawlader (2006) [78] experimentally and theoretically investigated flat plate, finned and v-corrugated air heaters in an effort to improve the performance of conventional air heaters. Collectors were also tested in double pass mode to investigate the extent of improvement in efficiency that could be achieved without increasing the collector size or cost. A series of experiments were conducted, based on the ASHRAE standard, under climatic conditions of Singapore. The performance of all three collectors was examined over a wide range of operating and design conditions. The v-corrugated collector was found to be the most efficient collector and the flat plate collector to be the least efficient.

Kareem et al. (2017) [79] investigated the performance efficiencies of multi-pass solar collector. Integration of solar collector unit and drying cabinet has been done to achieve MSCS. Repeated full-scale tests of MSCS for drying purpose have been conducted. Screw-pine has been dried within 28 h and its moisture content has been reduced from 74.5% to 4%. The study has achieved an average thermal collector, pickup, drying and exergy efficiencies of 58.73%, 66.95%, 36.04% and 27.23-550 86.82%, respectively. In addition, the system operation has been extended with the help of porous matrix that has enhanced the system performance by a range of 5-8%. The economic analysis of the system has indicated MSCS as a low risk project with a payback period of 0.75 year. The system has successfully eliminated the burning stage of processing the screw-pine through traditional drying method. This study is open to further study on enhancement of the thermal energy saving capacity.

Karim and Hawlader (2004) [80] performed an experimental study of three types of solar air collectors, namely flat plate, finned and v-corrugated, towards achieving an efficient design of air collector suitable for a solar dryer. A series of experiments were conducted, based on the ASHRAE standard, under Singapore climatic conditions. The performance of all three collectors was examined over a wide range of operating and design conditions. The improvement in efficiency for the double pass mode was most significant in the flat plate collector and least in the v-groove collector.

Al-damook (2017) [81] conducted experimental and theoretical studies to evaluate the thermal performance of an unglazed solar air collector featuring a perforated absorber flat plate under western Iraq environment weather conditions in Ramadi city. This work was carried out as the first such study in Iraq. The collector was inclined to 90° on the horizontal so that it can be easily placed on the wall of a building and to minimize its cost and weight. The thermal performance and economic characteristics of the collector were compared with other heating systems. The major results show that this type of collector offers advantages in economy and thermal performance under western Iraq climate conditions during both clear and cloudy winter days. In addition, the perforated flat plate absorber was effective and the UTC is effective in lowering both life cycle cost and energy used.

5. Conclusion

The topic is of paramount importance. Solar energy collectors are employed in several sectors and in very diverse fields. The improvement in their performance has been and is still of major concern to theorists and practitioners. The issue of exchanging heat between the caloporting fluid (air) and the absorber within a solar collector relies mainly on the value of the heat transfer coefficient. This coefficient is a mine of factors that affect the heat exchange between working fluid and heated surfaces. Therefore, it is an ambitious attempt to work on such a topic. In this study, we reviewed the different configurations of flat plate solar air collectors by highlighting three main groups: single-pass solar air collectors, double-pass solar air collectors, and multi-pass solar air collectors. We showed the various parameters in the design of solar energy collectors on which it is possible to act to enhance the thermal transfer phenomenon between the caloporting air and the absorber-plate, and thus to favor the energetic efficiency while assuring an optimal temperature augmentation. The investigations on different models and configurations with various heat transfer enhancement strategies of solar energy collectors were shown in various stages, i.e., modelling, control, measurement, and visualization of field or flow of air, determination of the heat transfer, control of friction loss and pressure drop, and evaluation of the thermal performance by the measurement of the augmentation in the temperature of the working fluid at a given solar irradiance and under given flow rate. We concluded this review by identifying the various applications possible for the solar air collectors such as heating and cooling of houses, drying agricultural food materials, and water desalination process.

References

[1] Ramani, B. M., Gupta, A., and Kumar, R., Performance of a double pass solar air collector, *Solar Energy*, 84, 2010, 1929-1937.

[2] Deng, J., Yang, X., Yang, M., and Wang, Z., Experimental study of a single-pass flat plate solar air collector with severe dust deposition on the transparent glass cover, *Energy Procedia*, 70, 2015, 32-40.

[3] Moss, R. W., Henshall, P., Arya, F., Shire, G. S. F., Eames, P. C., and Hyde, T., Simulator testing of evacuated flat plate solar collectors for industrial heat and building integration, *Solar Energy*, 164, 2018, 109-118.

[4] Zhu, T., Diao, Y., Zhao, Y., and Ma, C., Performance evaluation of a novel flat-plate solar air collector with micro-heat pipe arrays (MHPA), *Applied Thermal Engineering*, 118, 2017, 1-16.

[5] Lingayat, A., Chandramohan, V. P., and Raju, V. R. K., Numerical analysis on solar air collector provided with artificial square shaped roughness for indirect type solar dryer, *Journal of Cleaner Production*, 2018, doi: 10.1016/j.jclepro.2018.04.130.

[6] Abuşka, M., and Şevik, S., Energy, exergy, economic and environmental (4E) analyses of flat-plate and V-groove solar air collectors based on aluminium and copper, *Solar Energy*, 158, 2017, 259-277.

[7] Saedodin, S., Zamzamian, S. A. H., Eshagh Nimvari, M., Wongwises, S., and Javaniyan Jouybari, H., Performance evaluation of a flat-plate solar collector filled with porous metal foam: Experimental and numerical analysis, *Energy Conversion and Management*, 153, 2017, 278-287.

[8] Hernández, A. L., and Quiñonez, J. E., Experimental validation of an analytical model for performance estimation of natural convection solar air heating collectors, *Renewable Energy*, 117, 2017, 202-216.

[9] Rajaseenivasan, T., Srinivasan, S., and Srithar, K., Comprehensive study on solar air heater with circular and V-type turbulators attached on absorber plate, *Energy*, 88, 2015, 863-873.

[10] Abuşka, M., Energy and exergy analysis of solar air heater having new design absorber plate with conical surface, *Applied Thermal Engineering*, 131, 2018, 115-124.
[11] Li S., Wang H., Meng, X., and Wei X., Comparative study on the performance of a new solar air collector with different surface shapes, *Applied Thermal Engineering*, 114, 2017, 639-644.
[12] Ghiami, S., and Ghiami, A., Comparative study based on energy and exergy analyses of a baffled solar air heater with latent storage collector, *Applied Thermal Engineering*, 133, 2018, 797-808.
[13] Chen, G., Doroshenko, A., Koltun, P., and Shestopalov, K., Comparative field experimental investigations of different flat plate solar collectors, *Solar Energy*, 115, 2015, 577-588.
[14] Kabeel, A. E., Khalil, A., Shalaby, S. M., and Zayed, M. E., Improvement of thermal performance of the finned plate solar air heater by using latent heat thermal storage, *Applied Thermal Engineering*, 123, 2017, 546-553.
[15] Kalaiarasi, G., Velraj, R., and Swami, M. V., Experimental energy and exergy analysis of a flat plate solar air heater with a new design of integrated sensible heat storage, *Energy*, 111, 2016, 609-619.
[16] Mohammadi, K., and Sabzpooshani, M., Comprehensive performance evaluation and parametric studies of single pass solar air heater with fins and baffles attached over the absorber plate, *Energy*, 57, 2013, 741-750.
[17] Mohammadi, K., and Sabzpooshani, M., Appraising the performance of a baffled solar air heater with external recycle, *Energy Conversion and Management*, 88, 2014, 239-250.
[18] Bayrak, F., Oztop, H. F., and Hepbasli, A., Energy and exergy analyses of porous baffles inserted solar air heaters for building applications, *Energy and Buildings*, 57, 2013, 338-345.
[19] Chabane, F., Moummi, N., and Benramache, S., Experimental study of heat transfer and thermal performance with longitudinal fins of solar air heater, *Journal of Advanced Research*, 5(2), 2014, 183-192.
[20] Peng, D., Zhang, X., Dong, H., and Lv K., Performance study of a novel solar air collector, *Applied Thermal Engineering*, 30, 2010, 2594-2601.
[21] Hu, J., Sun, X., Xu, J., and Li, Z., Numerical analysis of mechanical ventilation solar air collector with internal baffles, *Energy and Buildings*, 62, 2013, 230-238.
[22] Youcef-Ali, S., and Desmons, J. Y., Numerical and experimental study of a solar equipped with offset rectangular plate fin absorber plate, *Renewable Energy*, 31, 2006, 2063-2075.
[23] Kabeel, A. E., Hamed, M. H., Omar, Z. M., and Kandeal, A. W., Influence of fin height on the performance of a glazed and bladed entrance single-pass solar air heater, *Solar Energy*, 162, 2018, 410-419.
[24] Deng, J., Yang, M., Mac, R., Zhu, X., Fan, J., Yuan, G., and Wang, Z., Validation of a simple dynamic thermal performance characterization model based on the piston flow concept for flat-plate solar collectors, *Solar Energy*, 139, 2016, 171-178.
[25] Ben Slama, R., The air solar collectors: Comparative study, introduction of baffles to favor the heat transfer, Solar Energy, 81, 2007, 139-149.
[26] Baccoli, R., Mastino, C. C., Innamorati, R., Serra, L., Curreli, S., Ghiani1, E., Ricciu, R., and Marini, M., A mathematical model of a solar collector augmented by a flat plate above reflector: Optimum inclination of collector and reflector, *Energy Procedia*, 81, 2015, 205-214.
[27] Priyam, A., and Chand, P., Effect of wavelength and amplitude on the performance of wavy finned absorber solar air heater, *Renewable Energy*, 119, 2018, 690-702.
[28] Manjunath, M. S., Vasudeva Karanth, K., and Yagnesh Sharma, N., Numerical investigation on heat transfer enhancement of solar air heater using sinusoidal corrugations on absorber plate, *International Journal of Mechanical Sciences*, 138-139, 2018, 219-228.
[29] Priyam, A., and Chand, P., Thermal and thermohydraulic performance of wavy finned absorber solar air heater, *Solar Energy*, 130, 2016, 250-259.
[30] Yeh, H. M., Upward-type flat-plate solar air heaters attached with fins and operated by an internal recycling for improved performance, *Journal of the Taiwan Institute of Chemical Engineers*, 43, 2012, 235-240.
[31] Yeh, H. M., Ho, C. D., and Lin, C. Y., The influence of collector aspect ratio on the collector efficiency of baffled solar air heaters, *Energy*, 23(1), 1998, 11-16.
[32] Bekele, A., Mishra, M., and Dutta, S., Effects of Delta-Shaped Obstacles on the Thermal Performance of Solar Air Heater, *Advances in Mechanical Engineering*, 2011, Article ID 103502, 10 p.
[33] Alam, T., Saini, R. P., and Saini, J. S., Experimental investigation on heat transfer enhancement due to V-shaped perforated blocks in a rectangular duct of solar air heater, *Energy Conversion and Management*, 81, 2014, 374-383.
[34] Handoyo, E. A., Ichsani, D., Prabowo, and Sutardi, Numerical studies on the effect of delta-shaped obstacles' spacing on the heat transfer and pressure drop in v-corrugated channel of solar air heater, *Solar Energy*, 131, 2016, 47-60.
[35] Kumar, R., Chauhan, R., Sethi, M., and Kumar, A., Experimental study and correlation development for Nusselt number and friction factor for discretized broken V-pattern baffle solar air channel, *Experimental Thermal and Fluid Science*, 81, 2017, 56-75.
[36] Kumar, R., Chauhan, R., Sethi M., Sharma, A., and Kumar, A., Experimental investigation of effect of flow attack angle on thermohydraulic performance of air flow in a rectangular channel with discrete V-pattern baffle on the heated plate, *Advances in Mechanical Engineering*, 8(5), 2016, 1-12.
[37] Kumar, A., and Kim, M. H., Thermal hydraulic performance in a solar air heater channel with multi v-type perforated baffles, *Energies*, 9, 2016.
[38] Kumar, A., and Kim, M. H., CFD Analysis on the Thermal Hydraulic Performance of an SAH Duct with Multi V-Shape Roughened Ribs, *Energies*, 9, 2016, 9.

[39] Kumar, R., Kumar, A., Chauhan, R., and Maithani, R., Comparative study of effect of various blockage arrangements on thermal hydraulic performance in a roughened air passage, *Renewable and Sustainable Energy Reviews*, 81, 2018, 447-463.
[40] Hematian, A., and Bakhtiari, A. A., Efficiency analysis of an air solar flat plate collector in different convection modes, *International Journal of Green Energy*, 12(9), 2015, 881-887.
[41] Amraoui, M. A., and Aliane, K., Three-dimensional analysis of air flow in a flat plate solar collector, *Periodica Polytechnica Mechanical Engineering*, 62(2), 2018, 126-135.
[42] Alam, T., and Kim, M. H., Performance improvement of double-pass solar air heater - A state of art of review, *Renewable and Sustainable Energy Reviews*, 79, 2017, 779-793.
[43] Sun, C., Liu Y., Duan, C., Zheng, Y., Chang, H., and Shu, S., A mathematical model to investigate on the thermal performance of a flat plate solar air collector and its experimental verification, *Energy Conversion and Management*, 115, 2016, 43-51.
[44] Nowzari, R., Mirzaei, N., and Aldabbagh, L. B. Y., Finding the best configuration for a solar air heater by design and analysis of experiment, *Energy Conversion and Management*, 100, 2015, 131-137.
[45] Yeh H. M., and Ho C. D., Downward-type solar air heaters with internal recycle, *Journal of the Taiwan Institute of Chemical Engineers*, 42, 2011, 286-291.
[46] Ho, C. D, Hsiao, C. F., Chang, H., and Tien, Y. E., Investigation of device performance for recycling double-pass V-corrugated solar air collectors, *Energy Procedia*, 105, 2017, 28-34.
[47] Gonzáleza, S. M., Larsen, S. F., Hernández, A., and Lesino, G., Thermal evaluation and modeling of a double-pass solar collector for air heating, *Energy Procedia*, 57, 2014, 2275-2284.
[48] Hassan, H, and Abo-Elfadl, S, Experimental study on the performance of double pass and two inlet ports solar air heater (SAH) at different configurations of the absorber plate, *Renewable Energy*, 116(A), 2018, 728-740.
[49] Ramani, B. M., Gupta, A., and Kumar, R., Performance of a double pass solar air collector, *Solar Energy*, 84, 2010, 1929-1937.
[50] Fudholi, A., Sopian, K., Ruslan, M. H., and Othman, M. Y., Performance and cost benefits analysis of double-pass solar collector with and without fins, *Energy Conversion and Management*, 76, 2013, 8-19.
[51] Fudholi, A., Sopian, K., Othman, M. Y., Ruslan, M. H., and Bakhtyar, B., Energy analysis and improvement potential of finned double-pass solar collector, *Energy Conversion and Management*, 75, 2013, 234-240.
[52] Lertsatitthanakorn, C., Khasee, N., Atthajariyakul, S., Soponronnarit, S., Therdyothin, A., and Suzuki, R. O., Performance analysis of a double-pass thermoelectric solar air collector, *Solar Energy Materials & Solar Cells*, 92, 2008, 1105-1109.
[53] Hernández, A. L., and Quiñonez, J. E., Analytical models of thermal performance of solar air heaters of double-parallel flow and double-pass counter flow, *Renewable Energy*, 55, 2013, 380-391.
[54] Aldabbagh, L. B. Y., Egelioglu, F., and Ilkan, M., Single and double pass solar air heaters with wire mesh as packing bed, *Energy*, 35, 2010, 3783-3787.
[55] Sopian, K., Alghoul, M. A., Alfegi, E. M., Sulaiman, M. Y., and Musa, E. A., *Renewable Energy*, 34, 2009, 640-645.
[56] Krishnananth, S. S., and Murugavel, K. K., Experimental study on double pass solar air heater with thermal energy storage, *Journal of King Saud University - Engineering Sciences*, 25, 2013, 135-140.
[57] Ravi, R. K., and Saini, R. P., Experimental investigation on performance of a double pass artificial roughened solar air heater duct having roughness elements of the combination of discrete multi V shaped and staggered ribs, *Energy*, 116, 2016, 507-516.
[58] Ho, C. D., Lin, C. S., Chuang, Y. C., and Chao, C. C., Performance improvement of wire mesh packed double-pass solar air heaters with external recycle, *Renewable Energy*, 57, 2013, 479-489.
[59] Ho, C. D., Chang, H., Lin, C. S., Chao, C. C., and Tien, Y. E., Analytical and experimental studies of wire mesh packed double-pass solar air heaters under recycling operation, *Energy Procedia*, 75, 2015, 403-409.
[60] Pramanik, R. N., Sahoo, S. S., Swain, R. K., Mohapatra, T. P., and Srivastava, A. K., Performance analysis of double pass solar air heater with bottom extended surface, *Energy Procedia*, 109, 2017, 331-337.
[61] Dhiman, P., Thakur, N. S., and Chauhan, S. R., Thermal and thermohydraulic performance of counter and parallel flow packed bed solar air heaters, *Renewable Energy*, 46, 2012, 259-268.
[62] Singh, S., and Dhiman, P., Thermal and thermohydraulic efficiency of recyclic-type double pass solar air heaters with fins and baffles, *Heat Transfer Engineering*, 37(15), 2016, 1302-1317.
[63] Orbegoso, E. M., Saavedra, R., Marcelo, D., and Madrid, R. L., Numerical characterisation of one-step and three-step solar air heating collectors used for cocoa bean solar drying, *Journal of Environmental Management*, 203(3), 2017, 1080-1094.
[64] Kareem, M. W., Habib, K., Sopian, K., and Irshad, K., Performance evaluation of a novel multi-pass solar air heating collector, *Procedia Engineering*, 148, 2016, 638- 645.
[65] Kareem, M. W., Gilani, S. I., Habib, K., Irshad, K., and Saha, B. B., Performance analysis of a multi-pass solar thermal collector system under transient state assisted by porous media, *Solar Energy*, 158, 2017, 782-791.
[66] Chen, W., and Liu, W., Numerical analysis of heat transfer in a composite wall solar-collector system with a porous absorber, *Applied Energy*, 78, 2004, 137-149.
[67] Jain, D., and Tiwari, G. N., Modeling and optimal design of ground air collector for heating in controlled environment greenhouse, *Energy Conversion and Management*, 44, 2003, 1357-1372.
[68] Hatami, N., and Bahadorinejad, M., Experimental determination of natural convection heat transfer coefficient in a vertical flat-plate solar air heater, *Solar Energy*, 82, 2008, 903-910.
[69] Yang, M., Yang, X., Li X., Wang, Z., and Wang, P., Design and optimization of a solar air heater with offset strip fin absorber plate, *Applied Energy*, 113, 2014, 1349-1362.

[70] Kabeel, A. E., Solar powered air conditioning system using rotary honeycomb desiccant wheel, *Renewable Energy*, 32, 2007, 1842-1857.

[71] Jain, D., and Jain, R. K., Performance evaluation of an inclined multi-pass solar air heater with in-built thermal storage on deep-bed drying application, *Journal of Food Engineering*, 65, 2004, 497-509.

[72] Madhlopa, A., Jones, S.A., and Saka, J. D. K., A solar air heater with composite-absorber systems for food dehydration, *Renewable Energy*, 27, 2002, 27-37.

[73] Bennamoun, L., and Belhamri, A., Design and simulation of a solar dryer for agriculture products, *Journal of Food Engineering*, 59, 2003, 259-266.

[74] Janjai, S., Srisittipokakun, N., and Bala, B. K., Experimental and modelling performances of a roof-integrated solar drying system for drying herbs and spices, *Energy*, 33, 2008, 91-103.

[75] Kareem, M. W., Habib, K., Ruslan, M. H., and Saha, B. B., Thermal performance study of a multi-pass solar air heating collector system for drying of Roselle (Hibiscus sabdariffa), *Renewable Energy*, 113, 2017, 281-292.

[76] Ben-Amara, M., Houcine, I., Guizani, A. A., and Maalej, M., Efficiency investigation of a new-design air solar plate collector used in a humidification-dehumidification desalination process, *Renewable Energy*, 30, 2005, 1309-1327.

[77] Moss, R. W., Shire, G. S. F., Henshall, P., Eames, P. C., Arya, F., and Hyde, T., Optimal passage size for solar collector microchannel and tube-on-plate absorbers, *Solar Energy*, 153, 2017, 718-731.

[78] Karim, M. A., and Hawlader, M. N. A, Performance investigation of flat plate, v-corrugated and finned air collectors, *Energy*, 31, 2006, 452-470.

[79] Kareem, M. W., Habib, K., Sopian, K., and Ruslan, M. H., Multi-pass solar air heating collector system for drying of screw-pine leaf (Pandanus tectorius), *Renewable Energy*, 112, 2017, 413-424.

[80] Karim, M. A., and Hawlader, M. N. A, Development of solar air collectors for drying applications, *Energy Conversion and Management*, 45, 2004, 329-344.

[81] Al-damook, A., Experimental evaluation of an unglazed solar air collector for building space heating in Iraq, *Renewable Energy*, 112, 2017, 498-509.